

Evaluating on-farm methods for estimating gas emissions and quantifying risk of disease
transmission for livestock barns

A Thesis

SUBMITTED TO THE FACULTY OF

UNIVERSITY OF MINNESOTA

BY

Anna M. Warmka

IN PARTIAL FULFILLMENT OF THE REQUIREMENTS

FOR THE DEGREE OF

MASTER OF SCIENCE

Dr. Erin Cortus

August 2023

Acknowledgements

First, I would like to thank Dr. Erin Cortus for her encouragement and support in both my undergraduate and graduate programs and research. She challenged me to always think critically and embrace the many ups and downs in this field of research. I feel grateful to have spent the last several years conducting research under her supervision. I am also thankful to Dr. Bo Hu and Dr. Melissa Wilson for reviewing my thesis work and providing valuable comments for improvement. I have appreciated working with Noelle Soriano and Dr. Baitong Chen in both the lab and field; they always made the long days and travel enjoyable. I am grateful to the farm cooperators who allowed us to sample and their farms, assisted in data collection, and provided their insights during the sampling periods. I am also thankful to the Livestock and Environmental Engineering group (Dr. Kevin Janni, Dr. Abby Shuft, Nancy Bohl Bormann, Dr. Jiayu Li, Matt Belanger, Dr. Chuck Clanton, Nohhyeon Kwak), Dr. Sally Noll, and David Schmidt for their help and suggestions for various parts of my projects. I would like to thank all my friends who have supported me through my MS program. Finally, I would like to thank my Mom, Dad, Robert, and Lauren for their support and curiosity in anything I choose to pursue.

Abstract

The need for producers to demonstrate the environmental and economical sustainability of their operations is driven by several stakeholder and consumer groups, creating a call for methods to accurately estimate gas emissions and quantify risk of disease transmission. In this work, I first provide background on the mechanisms of gas emissions from deep-pit swine operations and a summary of current emission estimation strategies in the literature. Next, I present one thesis project demonstrating the opportunities and limitations to applying a mass balance approach to estimate methane and ammonia emissions from deep-pit swine barns. Through this project, different mass balance approaches are evaluated against each other and typical emission modeling approaches. Findings from this project show that there are limitations to the application of a mass balance approach in swine barns, particularly related to in-barn sample collection and data availability. Then, I present a second thesis project identifying opportunities and limitations to using a fluorescent gel as a proxy for disease transfer in biosecurity research. In this project, I present a method to quantify the luminance of the fluorescent gel and investigate the factors important in measuring the transfer of gel from one surface to another. Findings from these two projects provide a framework for the methods needed to conduct research in gas emissions and biosecurity in livestock operations. Understanding the current state and limitations of these methods is important to consider when applying them to future research, and the current limitations presented provide an outline for future work needed in these fields.

Table of Contents

Acknowledgements.....	i
Abstract.....	ii
Table of Contents.....	iii
List of Tables.....	vii
List of Figures.....	viii
Chapter 1: Introduction.....	1
Chapter 2: Overview of Mechanisms of Gas Production and Release and Review of Current Emission Estimation Strategies in Livestock Systems.....	4
2.1 Mechanisms of Methane Production and Release.....	4
2.1.1 Enteric Fermentation.....	4
2.1.2 Manure Production and Storage.....	6
2.2 Mechanisms of Ammonia Production and Release.....	8
2.2.1 Urine Excretion and Ammonia Volatilization.....	9
2.2.2 Manure Production and Storage.....	11
2.3 Mechanisms of Carbon Dioxide Production and Release.....	12
2.3.1 Animal Respiration.....	12
2.3.2 Manure Production and Storage.....	13

2.4 Mechanisms of Nitrous Oxide Production and Release	14
2.4.1 Manure Production and Storage.....	14
2.5 Emission Estimation Strategies.....	17
2.5.1 Aerial Sampling	18
2.5.2 Material Mass Balance Approach.....	20
2.5.3 Modeling Approaches.....	22
Chapter 3: Applying a Mass Balance Approach to Minnesota Deep-Pit Swine Barns to Estimate Methane and Ammonia Emissions	25
3.1 Abstract.....	25
3.2 Introduction.....	26
3.3 Materials and Methods.....	28
3.3.1 Site Descriptions	28
3.3.2 Sample Collection Methods.....	32
3.3.3 Material Mass Balance Methods.....	34
3.3.4 Model Comparison Methods.....	37
3.4 Results and Discussion	40
3.4.1 Mass Distribution.....	40
3.4.2 Cumulative VS and N losses.....	43

3.4.3 Total CH ₄ and NH ₃ Emission Estimates	47
3.4.4 Generalized Linear Model for CH ₄ Emission Estimates	49
3.4.5 Model Comparisons for CH ₄ and NH ₃	53
3.5 Conclusion	56
3.6 Acknowledgements.....	57
Chapter 4: Opportunities and Methods for Using Fluorescent Gel as a Proxy for Pathogen Transfer in Biosecurity Research.....	58
4.1 Abstract.....	58
4.2 Introduction.....	59
4.3 Materials and Methods.....	62
4.3.1 Test Series 1 Mass over Time	64
4.3.2 Test Series 2 Luminance over Time	65
4.3.3 Test Series 3 Luminance Density Threshold	65
4.3.4 Test Series 4 Transferability of Wet Gel	67
4.3.5 Test Series 5 Transferability of Dried Gel.....	68
4.4 Results.....	69
4.4.1 Test Series 1 Mass over Time	69
4.4.2 Test Series 2 Luminance over Time	70

4.4.3 Test Series 3 Luminance Density Threshold	71
4.4.4 Test Series 4 Transferability of Wet Gel	73
4.4.5 Test Series 5 Transferability of Dried Gel.....	76
4.5 Discussion.....	78
4.6 Conclusion	80
4.7 Acknowledgements.....	81
Chapter 5: General discussion	82
5.1 Overall Summary	82
5.2 Limitations and Future Works	83
5.3 Conclusions.....	85
Bibliography	86
Appendix.....	99

List of Tables

Table 3.1 Mass balance components.	35
Table 3.2 Average measured and literature composition values for the 2023 sampling period of S1.....	41
Table A1. Camera settings used for Canon EOS Rebel SL1 in Test Series 1-5.....	99

List of Figures

Figure 3.1 Depiction of mass balance principles used in this study.	35
Figure 3.2 Flow chart of input values for each IPCC model iteration. Each iteration is labeled on the left in black boxes, and each input variable is labeled in blue boxes. Changes from default methods are denoted with red text.	38
Figure 3.3 Total mass flow distribution measured in the 2023 sampling period of S1.	40
Figure 3.4 Mass distribution of total VS measured in the 2023 sampling period of S1.	42
Figure 3.5 Mass distribution of total N measured in the 2023 sampling period for S1.	42
Figure 3.6 Cumulative VS loss for (a) 2023 S1 sampling period and (b) 2022 S2 sampling period for each balance approach.	44
Figure 3.7 Cumulative N loss for (a) 2023 S1 sampling period and (b) 2022 S2 sampling period for each balance approach.	45
Figure 3.8 CH ₄ emission estimates for each sampling period and balance approach. Average live animal masses and barn temperatures are also included under each sampling period.	48
Figure 3.9 NH ₃ emission estimates for each sampling period and balance approach. Average live animal masses and barn temperatures are also included under each sampling period.	48

Figure 3.10 Conventional mass balance CH ₄ estimates and GLM CH ₄ estimates by average live animal mass. Values are categorized by site.....	50
Figure 3.11 KZ mass balance CH ₄ estimates and GLM CH ₄ estimates by average live animal mass. Values are categorized by site.....	51
Figure 3.12 DBW mass balance CH ₄ estimates and GLM CH ₄ estimates by average live animal mass. Values are categorized by site.....	52
Figure 3.13 DBW mass balance CH ₄ estimates and GLM CH ₄ estimates by average barn temperature. Values are categorized by site.	53
Figure 3.14 Total CH ₄ emission estimates from each balance approach and model for all sampling periods.	54
Figure 3.15 Total NH ₃ emission estimates from each balance approach and model for all sampling periods.	55
Figure 4.1 Least square mean estimates of average evaporation rates for interactions between material and circle diameter. Vertical standard error bars are 0.00012 g min ⁻¹ . Letters above bars denote significant differences.	70
Figure 4.2 Least square mean estimates of luminance for interactions between material and circle diameter. Vertical standard error bars are 1.529 cm ⁻² . Letters above bars denote significant differences.....	71
Figure 4.3 The average luminance density values versus mass for each material (n=3), along with the fitted curves for each material. Average corrected luminance densities of	

38.4 cm ⁻² and 34.8 cm ⁻² for 0.2 g and 0.5 g, respectively for a rubber surface were excluded to highlight the results from 0 to 0.1 g. Horizontal and vertical bars indicate the standard error for each material and mass combination.....	73
Figure 4.4 The change in luminance least square mean estimates for each initial mass and circle diameter combination. Vertical standard error bars are included, and letters above bars denote significant differences.....	74
Figure 4.5 The least square mean estimates for mass loss from the source surface in wet gel transfer tests for combinations of material and circle diameter (a), material and initial mass (b), and initial mass and circle diameter (c). Vertical standard error bars are included, and letters above bars denote significant differences.	75
Figure A1. Graphical depiction of manure sampling methods.	99
Figure A2. Curtained table model constructed from wood without (a) and with (b) curtains made from blackout fabric lining. The fabric was secured using Velcro strips. The smaller hole was used for the UV light and the larger hole for the camera lens.	100
Figure A3. The image analysis process to quantify the fluorescent luminance and the area containing fluoresced pixels for a circle of Glogerm™ gel on a paper, using ImageJ; method adapted from Schindelin et al. (2012).....	100

Chapter 1: Introduction

There is increasing pressure from consumers for producers to demonstrate sustainability in their livestock operations. Environmental sustainability metrics are often presented in terms of the resources used or impacted in the production of a product. This is, in a way, a measure of efficiency. This efficiency is driven by both reduction in total gaseous emissions and reduction of animal losses through disease prevention. These metrics can be applied at broad national or regional scales, but are also important at farm-level for decision making. Research in both areas leads to better quantification of changes in sustainability metrics at the farm level through implementation of individual actions to reduce GHG production or improve animal health.

Each livestock operation is unique in its combination of location, species, housing structure, manure management methods, and biosecurity protocols; variability also exists within a single operation based on season, animal size, and animal activity. These large variations cause difficulty in capturing the characteristics of a specific operation with simplistic models or methods. There is a lack of standard methods for quantifying both GHG emissions and risk of disease spread from the livestock environment.

Some gases of concern from livestock operations include methane (CH_4), carbon dioxide (CO_2), nitrous oxide (N_2O), and ammonia (NH_3). Global warming potential (GWP) is often used to describe the relative warming intensity of greenhouse gases. The most abundant greenhouse gas in the atmosphere is CO_2 , which has a GWP of 1, while CH_4 has

a GWP of 21, meaning it is 21 times more effective at trapping heat from the sun in the atmosphere than CO₂, and N₂O has a GWP of 310 (Solomon et al., 2007). Ammonia is a non-greenhouse gas of concern. Atmospheric NH₃ is a precursor to atmospheric PM_{2.5} and PM₁₀ formation. Particulate matter strongly influences light scattering in the atmosphere, affecting atmospheric visibility and radiative forcing balance on all climate scales (Koziel et al., 2006). Additionally, PM_{2.5}, or particles less than 2.5 micrometers in diameter, can penetrate deeply into the human lung, irritate and corrode the alveolar wall, and impair lung function (Xing et al., 2016). Accurate quantification of emission rates of these gases from livestock operations can help researchers and producers better understand the influence these operations are having on the amount of these gases in the atmosphere.

Along with reduction of gaseous production from the livestock environment, prevention of disease transmission is a crucial factor in increasing livestock environmental and economic sustainability. Biosecurity is the suite of steps taken to reduce and prevent the spread of disease; biosecurity protocols vary greatly between species, housing types, and operation locations. For the protection of the affected industry, models or proxies are used for demonstration and quantification of transmission and exposure risk. Both within and outside of agricultural settings, fluorescing products have been used as pathogen proxies (Call et al., 2017; Conover & Gibson, 2017; Maitland et al., 2013). While these products are easily applied for demonstration purposes, there are no standard methods for consistently quantifying their fluorescence and relating it back to transmission rates or exposure risks.

In order to improve the credibility and reproducibility of results in both livestock emission and biosecurity research, more standardized approaches for farm-level applications are necessary. The objectives of this thesis were to: (1) evaluate methane and ammonia emissions from deep-pit swine barns using a material mass balance approach and compare emissions calculated through a mass balance approach to other emission estimation models, and (2) evaluate the properties for the fluorescent substance Glo Germ gel and identify important factors affecting the ability to quantify Glo Germ gel transfer from one surface to another. The next chapter will provide background on the mechanisms of gas release from deep-pit swine barns and an overview of emission estimation strategies in the literature.

Chapter 2: Overview of Mechanisms of Gas Production and Release and Review of Current Emission Estimation Strategies in Livestock Systems

In order to understand how gas emissions can be estimated from a farm, an understanding of gas generation from sources and release into the free airstream is crucial. This literature review describes how the gases of interest are generated and the mechanisms by which they transported from the source to the free airstream. Relevant factors affecting gas generation and emission rates are also covered. To better understand the application of emission estimation to livestock systems, current estimation strategies are also reviewed.

2.1 Mechanisms of Methane Production and Release

Methane (CH₄) production and emission from growing swine can be categorized into two sources: (1) emissions related to enteric fermentation and (2) emissions from manure production and storage.

2.1.1 Enteric Fermentation

Enteric fermentation accounts for approximately 14% of total methane emissions from growing swine (Grossi et al., 2019; MacLeod et al., 2018). Enteric fermentation is the digestive process in which carbohydrates are broken down by microorganisms into simple molecules to be absorbed into the blood stream of the animal (Jørgensen et al., 2011). Enteric CH₄ is produced by swine from the consumption of organic matter and subsequent anaerobic digestion via bacteria in the digestive tract (Philippe & Nicks, 2015). The majority of carbohydrates are digested by endogenous enzymes in the small intestine,

but dietary fiber is fermented in the lower hindgut, resulting in production of short chain fatty acids, carbon dioxide (CO₂), hydrogen (H₂) and CH₄ gases, urea, and heat. Additional H₂ is also produced in the stomach and small intestine from microorganisms (Jørgensen et al., 2011).

Feed composition and intake are the most influential factors on enteric CH₄ production. Swine feeds generally differ in organic matter contents and digestibility at different growth stages. For confined, growing swine, feed digestibility is generally between 80 and 90 percent (IPCC et al., 2019). Feed digestibility influences the rate of passage of feed in the digestive tract, influencing enteric CH₄ production. Previous experiments found the reduction of protein intake, and therefore reduced intake of neutral detergent fiber (NDF) and acid detergent fiber (ADF), reduced enteric CH₄ production in finishing pigs. Additionally, enteric CH₄ emissions have also been linked directly to the intake of non-starch polysaccharides (NSP), where increased NSP intake led to increased enteric CH₄ emissions (Moehn et al., 2005). Feed intake rates also directly influence CH₄ emissions. A low feed digestibility will result in lower feed intake, reducing growth but increasing CH₄ production per unit of growth; conversely, high digestibility feeds result in higher feed intake, increasing growth but decreasing CH₄ production per unit of growth (IPCC et al., 2019).

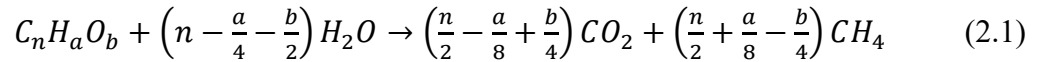
Other potential factors influencing enteric CH₄ production include environmental temperature and animal body weight. Some studies have shown a tendency for reduced enteric CH₄ production at lower environmental temperatures; general trends show

increasing CH₄ production with increasing animal body weight, however this trend is minor (Christensen & Thorbek, 1987; Noblet et al., 1989; Noblet & Shi, 1994). Other experiments have suggested that methanogenesis in pigs is fairly independent of live weight when feeding conditions remain constant (Jørgensen et al., 2011; Kirchgessner et al., 1991).

2.1.2 Manure Production and Storage

The significant proportion of CH₄ production and emission from swine stems from manure production and storage, accounting for approximately 86% of total methane emissions from growing swine (Grossi et al., 2019; MacLeod et al., 2018). After feed digestion and excretion, organic material is measured as the volatile solids (VS) content of the manure. Once excreted, VS begin to biodegrade through the process of anaerobic digestion (Ahring et al., 2003; Sweeten et al., 1981). Anaerobic digestion occurs in four stages: (1) hydrolysis; (2) acidogenesis; (3) acetogenesis; (4) methanogenesis. In hydrolysis, hydrolytic bacteria convert carbohydrates, lipids, and proteins into sugars, long chain fatty acids, and amino acids, respectively (Meegoda et al., 2018). Then in acidogenesis and acetogenesis, bacteria convert these easily digestible substrates into volatile fatty acids (VFAs), CO₂, and H₂ through microbial activity that increases the temperature of the manure and providing suitable conditions for methanogenesis to occur (Philippe & Nicks, 2015). Methanogenesis is an anaerobic respiration that generates methane as the result of metabolism (Lyu et al., 2018). Deep-pit liquid manure storages an anaerobic environment suitable for methanogenic bacteria to convert acetate, CO₂, and H₂

into CH₄ and CO₂, in a mixture known as biogas. The theoretical biogas yield through anaerobic can be described by equation 2.1 (Meegoda et al., 2018):



CH₄ production favors lack of oxygen, high temperatures, high levels of degradable organic matter, high moisture contents, low redox potentials, neutral pH, and C/N ratios between 15 and 30 (Amon et al., 2006; Kebreab et al., 2006; Møller et al., 2004; Philippe & Nicks, 2015).

Methanogenesis occurs strictly in anaerobic conditions, therefore occurring below the surface of the manure pit. Methane travels to the manure surface and is released through the process of ebullition, or the formation of CH₄ gas bubbles and its movement to the manure surface and transport across the liquid-air interface (Flesch et al., 2013; Park et al., 2010; Pescod, 1996). Ebullition occurs when CH₄ concentrations have exceeded their solubility in the anaerobic environment (Kaharabata et al., 1998). Short, intense bursts of CH₄ flux is also expected during manure agitation or pumping, as mechanical force and aeration allows the release of dissolved gas and trapped bubbles (Kaharabata et al., 1998; Leytem et al., 2017; VanderZaag et al., 2014). This immediate and intense increase in CH₄ release is often followed by a period of reduced CH₄ emissions for approximately one to two weeks (VanderZaag et al., 2019).

Similarly to enteric CH₄ emissions, diets rich in fiber increase CH₄ production in stored manure (Moehn et al., 2005; Philippe & Nicks, 2015). The Intergovernmental Panel

on Climate Change (IPCC) Guidelines for National Greenhouse Gas Inventories (IPCC et al., 2019) gives equation 2.2 to estimate the CH₄ emission factor for a given manure storage system based on excreted VS content (Tier 2):

$$EF = VS \times B_0 \times MCF \quad (2.2)$$

where *VS* is volatile solids excreted, *B*₀ is the maximum methane producing capacity, and *MCF* is the methane conversion factor. Additional equations are provided to estimate VS excreted based on feed intake and digestibility. The *B*₀ values vary by species and diet, defaulting to 0.48 m³ CH₄ kg⁻¹ VS for swine in North America. The *MCF* values are determined for specific manure management systems and climate zones of operation; the *MCF* values for deep-pit swine manure storage in Minnesota (cool temperature, moist climate zone) range from 6 percent for one month of storage to 31 percent for 12 months of storage (IPCC et al., 2019).

Other factors influencing CH₄ emissions from stored manure include barn temperature and ventilation rates, floor type (partially vs. fully slatted flooring), manure removal frequency, pit flushing frequency, and the use of pit treatment methods. Emissions are positively related to barn temperature and ventilation rates, and more frequent manure removal and pit flushing reduce emissions (Philippe & Nicks, 2015).

2.2 Mechanisms of Ammonia Production and Release

Approximately 70% of the nitrogen (N) in a pig's diet is excreted via feces (20%) or urine (50%) (Aarnink, 1997); the remainder (30%) is used by the pig for growth and

maintenance. The N in feces is mainly present in the form of amino acids, while the N in urine is present as urea (Aarnink, 1997). Swine obtain most of their amino acid requirements from protein in their feed consumed. The proteins, composed of amino acids, are released during digestion and absorption. It is assumed that all proteins contain 16 percent N, and in N calculations it is assumed that all N consumed comes in the form of protein, though this may not always be accurate (National Research Council, 1989).

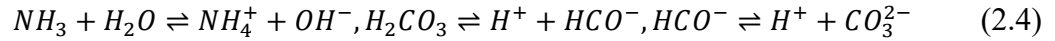
The bioavailability of amino acids differs for each unique feed composition. Grinding feed grains to decrease particle size can increase amino acid digestibility, and heating some ingredients during processing can also increase digestibility (Cargo-Froom, 2022). Other factors like protein solubility and levels of dietary fat and fiber can also influence digestibility (Lewis & Southern, 2000).

2.2.1 Urine Excretion and Ammonia Volatilization

Pigs excrete nitrogen in urine (in the form of urea) and feces (primarily in the form of protein) (Canh et al., 1997). Fecal matter alone can generally be considered a negligible ammonia source since nitrogen in the form of bacterial protein takes longer to convert to ammonia than urea (Cortus et al., 2010a). Urea undergoes enzymatic degradation in the presence of the enzyme urease, which is present in feces, to form NH_3 and carbonic acid (H_2CO_3) (eq. 2.3) (Colina et al., 2000; Mobley & Hausinger, 1989):



NH_3 and H_2CO_3 will both ionize in water to form ammonium (NH_4^+), hydrogen carbonate (HCO_3^-), and carbonate (CO_3^{2-}) (eq. 2.4) (Mobley & Hausinger, 1989):



Concentrations of NH_3 and NH_4^+ are often summed to find total ammoniacal nitrogen ($\text{NH}_4\text{-N}$) (Ni, 1999). The NH_3 will volatilize to the surrounding environment, with the volatilization rate depending on the $\text{NH}_4\text{-N}$ concentration in the puddle, pH, surface area, temperature, and air velocity over the surface (Colina et al., 2000; Cortus et al., 2008; Ni, 1999).

Experiments have indicated the conversion from urea to NH_3 and CO_2 begins immediately after urine is sprinkled onto a fouled floor surface; NH_3 emission rate tends to increase with time as the formation rate within the solution exceeds the volatilization rate, then peaks and begins to decrease as NH_3 formation slows down and ceases (Cortus et al., 2008; Elzing & Monteny, 1997a).

While air velocity over the puddle surface influences NH_3 volatilization rates, a study investigating NH_3 emissions in houses for fattening pigs with ceiling and floor ventilation systems found no significant differences between the two ventilation systems (Aarnink & Wagemans, 1997). Theoretical NH_3 volatilization via convective mass transfer can be described in equation 2.5 as (Olesen & Sommer, 1993):

$$E'_{\text{NH}_3} = k \cdot (C_g - C_a) \quad (2.5)$$

where E_{NH_3}' is the NH_3 volatilization per square meter of the NH_3 solution, k is the mass transfer coefficient, C_g is the NH_3 concentration in the gas boundary layer, and C_a is the NH_3 concentration in the atmosphere. In many cases, NH_3 concentration in the atmosphere is low compared to the concentration in the gas boundary layer and can be neglected. The concentration in the gas boundary layer can be calculated using Henry's law equation (eq. 2.6):

$$C_g = C_1 H \quad (2.6)$$

where C_1 is the NH_3 concentration in the liquid boundary layer and H is the Henry constant. The Henry constant is found based on temperature of the emitting surface (Aarnink & Elzing, 1998; Elzing & Monteny, 1997b; Hashimoto, 1972).

Urine puddles are significantly reduced in surface area and frequency with the use of slatted flooring, as there is an opportunity for urine to fall into the storage pit below. In general, NH_3 emission from buildings increases with the age of pigs and pen fouling, and higher feed intake leads to more N excreted in the urine, therefore enhancing NH_3 emission (Aarnink et al., 1995; Arogo et al., 2003; Hoeksma et al., 1992)

2.2.2 Manure Production and Storage

Pig manure is a mixture of urine and feces, containing undigested components of the diet, endogenous end products of digestion, and bacteria from the lower hindgut. The NH_3 exists in liquid manure in the form of ammonium ions (NH_4^+) and free ammonia (NH_3). The NH_3 in bulk manure can be transferred to the manure surface via mass diffusion

if there is a concentration gradient. Then, convective mass transfer, in the same manner as described for urine puddles, allows gaseous NH_3 at the manure surface to release into the free airstream (Ni, 1999; Ni et al., 2009). This mass transfer depends on both the transport properties and the dynamic characteristics of the flowing fluid (Welty et al., 1984). Release into the free airstream is also influenced by manure surface conditions, like the presence of a manure surface crust. A surface crust reduces mass and energy exchanges, increasing the resistance to NH_3 transport and contributing to a reduction in NH_3 emissions (Sommer et al., 2003).

2.3 Mechanisms of Carbon Dioxide Production and Release

Carbon dioxide (CO_2) originates from animal exhalation and manure storages.

2.3.1 Animal Respiration

The level of CO_2 exhalation depends on the physiological stage, body weight, production level, and feed intake of the animals in question (Philippe & Nicks, 2015). This CO_2 production relates to a respiratory quotient, or a ratio between the volume of CO_2 produced and the volume of oxygen consumed. Respiratory quotients have been reported in literature for varying pig growth stages, including a value of 1.10 for growing pigs (Atakora et al., 2011). The rate of CO_2 exhalation can also be estimated from animal heat production, corresponding to the energy used for maintenance, production, and thermoregulation (Noblet et al., 1989). Heat production should be estimated while taking into account the pig's body weight (BW), production level, and feed energy intake (CIGR, 2002). CO_2 exhalation as a function of BW has been modeled for swine in cases of a lack

of data (Brown-Brandl et al., 2004; Feddes & DeShazer, 1991; Müller & Schneider, 1985; Ni, Hendriks, et al., 1999; Pedersen et al., 2008; Philippe & Nicks, 2015; Van't Klooster & Heitlager, 1994).

2.3.2 Manure Production and Storage

In manure, CO₂ is produced from three processes: (1) rapid hydrolysis of urea into NH₃ and CO₂ via the enzyme urease; (2) anaerobic fermentation of organic matter into intermediate VFAs, CH₄, and CO₂; and (3) aerobic degradation of organic matter (Jeppsson, 2000; Møller et al., 2004; Wolter et al., 2004). For liquid manure, anaerobic processes are often considered the most prevalent source of CO₂, but contradictory results have also indicated that aerobic and anaerobic processes are of almost equal importance at a temperature of 20°C, while lower temperatures favor anaerobic processes (Møller et al., 2004; Ni, Vinckier, et al., 1999).

Carbon dioxide production in manure storage via anaerobic processes has already been described in the production of CH₄ and CO₂ as biogas. Additional CO₂ production is a byproduct of urea hydrolysis. In the first reaction of urea hydrolysis, NH₃ and carbamic acid (NH₂COOH) are formed. The carbamic acid eventually breaks down into NH₃ and CO₂ in aerobic conditions through the following reaction (eq. 2.7) (Ranjan & Singh, 2023):



Along with urea hydrolysis, aerobic decomposition by microbes utilizes organic matter/carbon sources in the manure and convert to CO₂ (Inbar et al., 1993). This CO₂

production is dependent on microbial activity in the manure, availability of carbon and nitrogen sources, and the environment of either aerobic or anaerobic conditions (Barrington et al., 2002; Bernal et al., 2009; Hu et al., 2018; Kirchmann & Witter, 1989). Transfer of CO₂ into the free airstream occurs primarily via convective mass transfer, as described for NH₃ transfer from bulk manure to the free airstream.

Ni et al. (1999) created the following mathematical model (eq. 2.8) to estimate the release of CO₂ from manure storage based on total pig weight, manure temperature, and ventilation rate:

$$Q = 295.5 \times 10^{-3} W + 4.5T + 232.4 \times 10^{-3}V - 462.5 \quad (2.8)$$

where Q [g h⁻¹] is estimated CO₂ release, W [kg] is the total weight of pigs, T [°C] is the manure temperature, and V [m³ h⁻¹] is the ventilation rate. This study determined average CO₂ release from manure to be 37.5% of that exhaled by animal respiration, significantly higher than previously reported values of less than 5% (Ni et al., 1999).

2.4 Mechanisms of Nitrous Oxide Production and Release

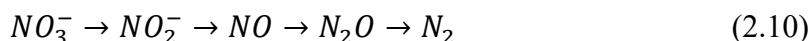
2.4.1 Manure Production and Storage

In finishing pigs, nitrous oxide (N₂O) originates solely from stored manure, formation occurring primarily from incomplete nitrification/denitrification processes performed by microorganisms to convert NH₃ into molecular nitrogen (N₂) (Philippe & Nicks, 2015). Nitrification, the process of converting NH₃ into nitrate (NO₃⁻), requires a

pH value above 5; during this process, N₂O is synthesized as a byproduct when there is a lack of oxygen or a nitrite accumulation (eq. 2.9) (Kebreab et al., 2006):

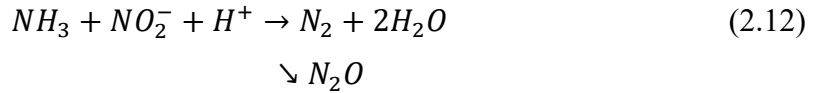
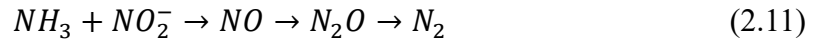


Denitrification, the reduction of NO₃⁻ into N₂ includes the production of many intermediate compounds, including nitrite (NO₂⁻), nitric oxide (NO), and N₂O (eq. 2.10) (Kebreab et al., 2006):



This process occurs under anaerobic conditions, and N₂O is produced when reduction to N₂ is incomplete. Conditions necessary for complete denitrification include the presence of facultative heterotrophic bacteria capable of carrying out the process, the availability of reductants, lack of oxygen, and high concentrations of NO₃⁻, NO₂⁻, or NO (Firestone & Davidson, 1989). The accumulation of N₂O through this process is favored in the presence of oxygen and low availability of degradable carbohydrates (Driemer & Van den Weghe, 1997; Poth & Focht, 1985).

N₂O production can also occur in other microbial pathways, including the nitrifier denitrification process and the anamox process. The nitrifier denitrification process is the oxidation of ammonium under aerobic conditions, while the anamox process is the oxidation of ammonium under anaerobic conditions; these processes occur through the following reactions, respectively (eq. 2.11 and 2.12) (Philippe & Nicks, 2015):



N₂O production can be influenced by different environmental factors like temperature, moisture, mixing, manure composition, redox potential, pH, substrate concentration gradients, etc. (Broucek, 2016). There is a strong correlation between N₂O emissions and manure temperature, with differing emission rates under summer and winter conditions (Jungbluth et al., 2001). As a soluble compound, N₂O is transferred into the free airstream primarily via convective mass transfer, as described for NH₃ transfer from bulk manure to the free airstream.

The IPCC Guidelines for National Greenhouse Gas Inventories provides methods for estimating direct and indirect N₂O emissions from stored manure. Equation 2.13 estimates direct N₂O emissions (Tier I) (IPCC et al., 2019):

$$N_2O = (N \cdot N_{ex} + N_{cdg}) \times EF \times \frac{44}{28} \quad (2.13)$$

where N is the number of head of livestock, N_{ex} is the average N excretion per head, N_{cdg} is the nitrogen input via co-digestate, and EF is the emission factor for direct N₂O emissions from the specified manure management system. IPCC provides default values for N_{ex} based on region and category of animal. This value for swine in North America is 0.39 kg N (1000 kg animal mass)⁻¹ day⁻¹. Default values are also provided for EF , based

on manure management system. This value of pit storage below animal confinements is $0.002 \text{ kg N}_2\text{O-N (kg N excreted)}^{-1}$.

2.5 Emission Estimation Strategies

There is increasing pressure from consumers, regulatory bodies, and incentive-based programs for air emission estimation in the livestock industry. However, accurate and reproducible emission values are difficult to measure for multiple reasons. There is no set “standard” method for measuring emissions from livestock barns of varying species, housing structures, and manure management methods. There are large variations between operations that can be difficult to capture with one defined method. The processes that influence gaseous emission production are complex and dynamic. Within a single operation, these emission values are influenced by species, housing type, season, environmental conditions, animal size and activity, and more.

Regardless of the challenges faced in emission estimation, several strategies have been used in previous research and reporting. Each strategy has its own set of benefits and limitations, giving researchers the flexibility to choose which strategy works best for their work. Strategies for barn emission estimation can be organized into three categories: aerial sampling, material mass balance approaches, and modeling approaches.

When choosing an emission estimation method for a mechanically ventilated barn system, there are three important considerations:

1. Measurement location: Emission estimates depend on defined boundaries set by the researcher, generally the whole barn, manure storages, or several sources within a barn. Measurement location becomes important because of spatial variabilities in air flow and gas concentration; measurement locations should be representative of the source area(s).
2. Measurement frequency: Temporal variations in airflow and gas concentrations are defined by measurement frequency. Measurement frequency methods allow researchers to identify seasonal or diurnal changes in emissions when desired.
3. Instrument sensitivity: Gas concentration measurements vary between the gas of interest and the measurement locations. It is important for any instruments used for measurement to support the range of gas measurements expected in the study.

2.5.1 Aerial Sampling

Aerial sampling methods include two main components: measurement of the difference between inlet and outlet gas concentrations, and estimation of exhaust fan ventilation rates. Emissions and emission rates can be estimated based on these two measurements. Previous research has shown large variation both spatially and temporally for these two measurements, both between operations and within the same operation (Fiedler et al., 2013; Groot Koerkamp et al., 1998; Hoff et al., 2006; Schauburger et al., 2013). Aerial sampling approaches are generally viable in all housing systems; however, it is important to choose the appropriate concentration and ventilation measurement methods,

considering the three important considerations previously mentioned and the project objectives.

Gas concentration measurement methods include either continuous or non-continuous aerial sampling. Continuous sampling methods include fluorescent, optical, and chemiluminescent instruments that allow for simultaneous sampling of multiple gases from a barn (Hristov et al., 2011). These instruments are useful for both long- and short-term studies, as they typically provide high frequency data. Non-continuous sampling methods include sample collection at locations in the barn with subsequent analysis in a lab. Some sample collection methods include the use of passive samplers, denuders, acid washing/gas scrubbing, or sampling bags (Hassouna et al., 2016). Subsequent lab analysis to determine gas concentrations include methods of gas chromatography, photoacoustic infrared absorption spectroscopy, differential optical absorption spectroscopy, and laser absorption spectroscopy (Hassouna et al., 2016; Hristov et al., 2011). Non-continuous sampling methods are often more time-consuming, but results provide high accuracy. These methods are often more suitable for long-term sampling to represent average values over a designated time period.

Ventilation rates can be measured using direct methods like an anemometer, or using indirect methods like a CO₂, humidity, or heat balance, or tracer gas methods (Chen et al., 2014; Demmers et al., 2001; Hassouna et al., 2016; Hinz & Linke, 1998). In mechanically ventilated barns, monitoring of fan operating stage and performance can also be used to find airflow values. Fan operation data should ideally be supplemented with

static differential pressure measurements across each barn wall with fans, and fan speed data can aid in describing fan efficiency (Jin et al., 2012; Wang-Li et al., 2013). Fan performance curves with respect to differential pressure are found in the field using a Fan Assessment Numeration System (FANS) unit (Gates et al., 2004).

One limitation of using an aerial sampling approach is the constraint of choosing sampling locations because of the spatial and temporal variabilities in emissions (Calvet et al., 2010). Aerial sampling methods only represent airflow and concentration values from limited areas, creating uncertainties from unaccounted areas and time periods. This uncertainty, combined with instrumental and procedural uncertainties, creates a large range of emission estimates observed in the literature (Qu et al., 2021). The use of gas sampling system can help reduce these uncertainties by being customized based on the objective of the project and by including several gas and airflow sampling locations.

2.5.2 Material Mass Balance Approach

The purpose of the material mass balance approach is to be adaptable to various housing systems to estimate emissions based on its main principle. The credibility of the mass balance approach depends on data accuracy and availability, and the frequency on inflows and outflows from the system (Hristov et al., 2011). This approach is an averaging approach and cannot predict temporal variations within short periods (Keener & Zhao, 2008). Data used in the mass balance approach represent a cumulative value of the compound of interest, making it more often used to estimate emissions over longer periods of time, including monthly, seasonally, and yearly estimates (De Boer & Wiersma, 2021;

Keener & Zhao, 2008; Yang et al., 2000). The mass balance method has limitations because certain balance parameters including animal growth, feed addition, and feed composition changes must be estimated (Phillips et al., 2001).

Advantages of the mass balance approach include no requirement for air sampling to estimate emissions. Measurement location considerations for this approach are dependent on the inflow and outflow streams accounted for in the system defined by the researcher. Location is related to sources of the compounds of interest in the balance. While some sources are easy to track, like livestock inventory and feed intake, others, especially manure production, are typically not regularly tracked by producers (Keener & Zhao, 2008). In most mass balance studies, manure mass flows are estimated (Coufal et al., 2006; De Boer & Wiersma, 2021; Li et al., 2010). This may influence the accuracy of overall emission estimates as manure is a significant source of many gases of interest.

Li et al. (2010) addressed the uncertainty of emission estimates obtained using mass balance approaches by comparing NH₃ emission estimates from a commercial turkey barn using a mass balance approach to results obtained via aerial sampling methods. This comparison discovered large differences between estimates using these two methods (Li et al., 2010). Other studies using the mass balance discuss this discrepancy and apply correction factors to adjust preliminary estimates. For example, a study by De Boer and Wiersma (2021) used an N balance supplemented with phosphorus (P) and potassium (K) balances to estimate emissions. Phosphorus and potassium are not volatilized or lost through leaching, so these balances can be used to correct the N balance for better accuracy

(De Boer & Wiersma, 2021). Another study, Keener and Zhao (2008), used an ash balance in tandem with an N balance to estimate NH₃ emissions from a poultry layer barn. Similar to P and K, ash does not volatilize, and in this study was used to track manure movement through the system. Accurate manure production estimates are essential to ensure accurate emission estimates through the mass balance approach because it is such a significant source for emissions.

2.5.3 Modeling Approaches

Modeling approaches for emission estimation can be categorized as emission factors, empirical models, and process-based models. Emission factors (EF) are the simplest model approach available. These factors describe the mass of pollutants released from livestock systems per unit of animal inventory. These estimates are broad and differ by housing types and species. Agencies like the IPCC or Environmental Protection Agency (EPA) often use emission factors for decision-making and creating baseline values for emission reduction goals (Doorn et al., 2002; Rigolot et al., 2010). Empirical models use simple regression equations based on measured data as model inputs (Jose et al., 2016). These models do not fully describe system behaviors and interactions, but describe relationships in line with mechanistic understanding (Adams et al., 2013; Korzukhin et al., 1996). Process-based models can be more comprehensive and incorporate mechanism explicitly, focusing on simulating detailed processes that describe system behavior directly (Adams et al., 2013). This level of detail makes process-based models ideal for estimating emissions at the farm level.

Past and ongoing research has worked to develop process-based and whole-farm models for emission estimation, particularly for NH_3 (Cortus et al., 2010a, 2010b; Li et al., 2012; Monteny et al., 1998; Rotz et al., 2014). Whole-farm models describe entire farm systems, incorporating processes like gas production from the animal and volatilization from the manure, as well as interactions between processes, and the effects of environmental conditions and management practices (Olesen et al., 2006; Rotz et al., 2014). These models can therefore be more comprehensive and specific in providing estimates at the farm level. In order to accurately predict gas emissions, process-based models often use empirical data as model inputs (Adams et al., 2013; Korzukhin et al., 1996). Model calibration and parameterization are important steps in model development, depending greatly on the availability and quality of data, which is the main limitation for this technique (Del Prado et al., 2013; Jose et al., 2016). All process-based models have inherent uncertainties depending on data availability, with varying levels of uncertainty for different models (Crosson et al., 2011). If these data are lacking, model predictions can be too general to be considered useful (Jose et al., 2016).

With the several approaches to emission estimation, there is a lack of standardization of methods, contributing to the variability identified in current gas emission inventory. Understanding and evaluating the emission estimation approach used is an important consideration when interpreting emission results and applying them to decision-making. Through the next chapter, this work applies material mass balance approaches for

estimating emissions from swine operations, as well as investigating modeled emission values. Specifically, this work:

1. Presents CH₄ and NH₃ emission estimates and estimation reliability from two finishing swine barns in Minnesota.
2. Compares material mass balance emission estimates to those calculated through modeling approaches.

Chapter 3: Applying a Mass Balance Approach to Minnesota Deep-Pit Swine Barns to Estimate Methane and Ammonia Emissions

3.1 Abstract

Producers are under pressure to demonstrate and document environmental sustainability. Responding to these pressures requires measurements to demonstrate greenhouse gas (GHG) emissions and/or changes over time. Methane (CH_4) and ammonia (NH_3) are primarily released from stored manure, but current emission inventories (models) do not account for all production and management systems. The purpose of this project was to track flows of nitrogen, volatile solids, and ash into and out of two deep-pit swine barns to estimate CH_4 and NH_3 emissions. Using a mass balance approach, volatile losses of nitrogen and volatile solids were estimated through simultaneous balances with ash (fixed solids). Through these methods, masses of feed consumed, manure produced, and animal growth were found to be the most influential balance variables. In general, CH_4 emissions were influenced significantly by live animal mass, with emissions increasing with live animal mass. In some instances, CH_4 emissions were also significantly influenced by average barn temperature, again with emissions increasing with barn temperature. Emission estimates for CH_4 and NH_3 using a mass balance approach were not comparable to emission modeling methods. This could lend to inaccuracies with the mass balance approach, or signify inaccuracies in the assumptions used for the model approaches. The work presented suggests a mass balance approach has potential for estimating CH_4 and NH_3 emissions from deep-pit swine barns, however this is dependent on data availability

and accuracy, as well as accuracy of the assumptions made throughout the sampling, measurement, and analysis processes.

3.2 Introduction

Methane (CH₄) and ammonia (NH₃) emissions from deep-pit swine barns pose detrimental effects on the environment and contribution to global warming. The release of CH₄ gas is of concern for its contribution to ozone formation in the troposphere and ozone degradation in the stratosphere (Noël et al., 2018; West & Fiore, 2005). Additionally, the global warming potential of CH₄ is 21 times that of CO₂, meaning it is 21 times more effective at trapping heat from the sun in the atmosphere than CO₂ (Solomon et al., 2007). The quantity of CH₄ produced globally from livestock accounts for approximately 35% of total anthropogenic CH₄ emissions (Gerber et al., 2013). Within these emissions, manure management comprises approximately 10%, with the pigs being the dominant species within this sources (~42%) (Gerber et al., 2013; Reay et al., 2018).

Atmospheric NH₃ poses a threat as it reacts with acidic gases in the air to form atmospheric particulate matter. Particulate matter strongly influences light scattering in the atmosphere, affecting atmospheric visibility and radiative forcing balance on all climate scales (Koziel et al., 2006). Additionally, PM_{2.5}, or particles less than 2.5 micrometers in diameter, can penetrate deeply into the human lung, irritate and corrode the alveolar wall, and impair lung function (Xing et al., 2016). Ammonia can also contribute to the acidification of soils and water bodies (Camargo & Alonso, 2006; Fangmeier et al., 1994; Ritz et al., 2004).

Emission estimation is difficult because there is no single instrument or standard method used to measure the release rate of gases from multiple sources within a livestock system. There are several current strategies for emission estimation, however no single strategy can provide reliable estimate across operations varying in housing systems, species, and management decisions. Use of a material mass balance approach is one option for emission estimation. In this research, a mass balance approach refers to emission estimation based on stocks and flows within a defined system boundary, where emissions are calculated based on losses of elemental components of the stocks and flows (Coufal et al., 2006). This approach has potential for application in several different housing systems.

The credibility of the mass balance approach depends on data accuracy and availability, and the frequency on inflows and outflows from the system (Hristov et al., 2011). Li et al. (2010) addressed the uncertainty of emission estimates obtained using mass balance approaches by comparing NH₃ emission estimates from a commercial turkey barn using a mass balance approach to results obtained via aerial sampling methods. This comparison discovered large differences between estimates using these two methods (Li et al., 2010). Other studies using the mass balance discuss this discrepancy and apply correction factors to adjust preliminary estimates. For example, a study by De Boer and Wiersma (2021) used an N balance supplemented with phosphorus (P) and potassium (K) balances to estimate emissions. Phosphorus and potassium are not volatilized or lost through leaching, so these balances can be used to correct the N balance for better accuracy (De Boer & Wiersma, 2021). Another study, Keener and Zhao (2008), used an ash balance

in tandem with an N balance to estimate NH_3 emissions from a poultry layer barn. Similar to P and K, ash does not volatilize, and this study was used to track manure movement through the system. Accurate manure production estimates are essential to ensure accurate emission estimates through the mass balance approach because it is such a significant source for emissions.

There are few resources available to estimate CH_4 and NH_3 emission at the farm level for deep-pit swine operations. Emission factors for CH_4 and NH_3 exist from the Intergovernmental Panel for Climate Change (IPCC) and U.S. Environmental Protection Agency (EPA) for swine (IPCC et al., 2019; U.S. EPA, 2020). These values, however, cannot account for variabilities between livestock operations or spatial and temporal variabilities within a single operation. Given the challenges of emission estimation methods for swine at the farm-level, the objectives of this study were to:

- (1) Use linear model analyses to evaluate the relationships of farm, barn temperature, and live animal mass with CH_4 and NH_3 emissions estimated via a material mass balance approach.
- (2) Compare CH_4 and NH_3 emissions calculated through a material mass balance approach to other estimation models.

3.3 Materials and Methods

3.3.1 Site Descriptions

Two swine finishing barns were sampled throughout the course of this study and will be referred to as S1 and S2.

3.3.1.1 S1 Site Description

Barn Layout and Ventilation

Barn S1 was a wean-finish barn located in Pipestone County, MN. This production scale research barn had two rooms, split down the middle in the east-west direction. The north room had dimensions of 59.4 meters by 15.2 meters, with fully slatted floors and a 2.6-meter pit depth; the south room had dimensions of 59.4 meters by 15.2 meters, with fully slatted floors and a 2.4 meter pit depth. Each room included 40 pens housing approximately 27 pigs per pen. Each pen had dimensions of approximately 2.7 meters by 7.0 meters.

The barn had mechanical ventilation, with a curtain on the west wall for tunnel ventilation mode in hot weather. Barn S1 sourced all water from a rural well with a water meter for each room. Water meter readings were recorded weekly for each room to track water usage. On site, the farm collected outdoor temperature data, and the nearest weather station was located 9.3 kilometers west of the site.

Animal Capacity and Diet

Each room housed 1,200 pigs in a turn. Each turn began with pigs between 6.4 and 7.3 kilograms and lasted between 154 and 160 days. The pigs were sent to market at approximately 131.5 kilograms. This barn cycled 2.1 turns per year on average. Barn S1 was a research barn, so pig breed varied for different trials. Between turns, 10 to 14 days were used for cleanout. During the times of sampling, four different feeds were used for

research trials, splitting the pens equally between each feed type. The trials at the times of sampling used no unique feed or diet additives.

For research purposes, there were detailed feed delivery records during all trials in this barn, indicating the weight of feed delivered to each pen and the minute it was delivered. Pig weights were measured and averaged weekly, and water meter readings for each room were recorded weekly.

Manure and Mortality Management Methods

Barn S1 used a deep-pit system, with a complete manure removal each year in October. No specific additives were used within the manure. Records existed from the two manure analyses done prior to the first sampling period. The barn recorded mortalities daily and uses on-site composting for mortality management.

3.3.1.2 S2 Site Description

Barn S2 was a grow-finish barn located in Nicollet County, MN, constructed in 2018. The barn consisted of two rooms, split down the middle in the east-west direction. Each room had dimensions of approximately 59.7 meters by 18.3 meters, with 2.4-meter ceilings, a fully slatted floor, and a 2.4-meter pit depth. A concrete wall separated the deep-pit space between the two rooms, with equalizing holes near the top of the wall. There were two rows of pens in each room with a center alley.

The barn was mechanically ventilated; a curtain opening on the east wall opened for tunnel ventilation in hot weather. In cold weather, air entered via soffits into the attic, and into the room through ceiling inlets.

Barn S2 supplied all water from a rural well water source, and a water meter was located on site. Water meter readings were recorded monthly to track water usage in the entire barn. On site, the farm collected outdoor temperature data and the temperature in each room, and the nearest weather station was located 10.6 kilometers northwest of the site.

Animal Capacity and Diet

Each room of this barn housed 1,500 pigs in a turn. Each turn started with approximately 22.7-kilogram pigs and lasted approximately 3 months. Pigs were sent to market at approximately 130 kilograms, in numerous loads over a three to four week span. Average pig weights were available at the start and end of each turn.

Wet-dry feeders were located in the center of each pen. A bulk bin supplied the feeders in each row of pens. The farm received multiple loads of feed each week, and maintained a record of load weights in the barn office.

Manure and Mortality Management

Barn S2 used a deep-pit system, with a complete manure removal each year in the fall for land application. A pit additive was used to prevent solid accumulation during sampling periods. Records existed from the two manure analyses done prior to the first

sampling period. The barn recorded mortalities daily and kept a running inventory of pigs in each room.

3.3.2 Sample Collection Methods

Sample collection was conducted over a five-week sampling period, with five total sampling days per period (one per week). Two sampling periods were conducted at both S1 and S2, once in the summer of 2022, and once in the spring of 2023. Sampling at S1 spanned the entirety of the barn, including both rooms; sampling at S2 however, was only done in the south room. On each sampling day, one composite manure sample was acquired and frozen until analysis. Composite manure samples were collected using a profile sampler made from PVC pipe and a rubber ball attached to a string (see figure A1 for graphical depiction). Profile samples were taken through the slatted floor at three locations across the manure pit, and all samples were mixed in a bucket before being transferred to the sampling container. The same three locations in each barn were used for every sampling day. Manure samples were sent to a commercial lab for analysis. Each sample was analyzed for moisture content, ash content, and total Kjeldahl nitrogen (TKN) content. Moisture and ash content were measured using sample drying and combustion processes, and TKN content was measured using digestion and a flow injection analyzer. These standard methods are described in Wilson & Cortus (2022).

Along with samples, manure production volume was also measured on each sampling day. At each of the three manure sampling points, a BOSCH GLM20 Blaze 65ft Laser Distance Measurer (Bosch USA, Farmington Hills, MI, USA) was used to find the

distance from the top surface of the slatted floor to the manure surface in the pit to the nearest inch. These three distances were averaged and used along with the pit dimensions to estimate total manure volume.

One feed sample was collected on each sampling day. Composite feed samples were collected by grabbing handfuls of feed directly out of feeder at various locations around the barn. For S2, equal amounts of all four feeds being used for research trials were collected and mixed thoroughly. Feed samples were sent to a commercial lab for analysis. Each sample was analyzed for moisture content, ash content, and TKN content. Moisture and ash content were measured using AOAC Official Method 942.05 (JAOAC, 1996). Total Kjeldahl nitrogen content was measured using AOAC Official Method 990.03 16th Edition, Ch 4 pg 18 (AOAC, 1995).

Weekly feed intake was estimated from data provided by the producers. For S1, feed delivery data was very detailed and provided minute-by-minute feed delivery for each pen in the barn, giving the assumed feed intake strong accuracy. For S2, feed delivery data was provided via invoices detailing feed delivery weights (in tons) and date of delivery. These data were then interpolated to estimate feed intake for each week.

A water sample was collected on the first day of each sampling period and assumed to stay consistent in content throughout the course of sampling. Water meter readings were provided by the producers when available. S1 water meter readings were provided weekly, separating the north and south rooms; S2 water meter readings were provided monthly and used to estimate weekly water consumption.

In each barn, a Kestrel DROP 2 (Kestrel Instruments, Boothwyn, PA, USA) was hung in the center of the room at approximately eye level. This instrument recorded temperature, relative humidity, and dew point inside the barn every 10 minutes throughout each sampling period.

Other data provided weekly from producers included the number of pigs currently housed in the building, the number of mortalities in the previous week, and any sales during the previous week. Finally, average pig weights were provided by producers when available. S1 pig weights were taken often over the course of sampling and were used to interpolate approximate weekly animal growth; S2 pig weights were taken at the beginning and end of the turn, so more rough estimation was used to approximate weekly animal growth. Moisture content, ash content, and TKN content for mortalities and animal growth were estimated using literature values (Okrouhlá et al., 2006).

3.3.3 Material Mass Balance Methods

Three mass balance methods were used for each sampling period. The goal of these mass balances was to estimate gaseous methane and ammonia emissions from each barn using their mass precursors, volatile solids (VS) and nitrogen (N), respectively. Movement of the components all mass balances is depicted in Figure 3.1. These methods estimated losses assumed to be gaseous emissions by utilizing the mass conservation principle: the sum of inputs should equal the sum of outputs and change in storage over a defined time period.

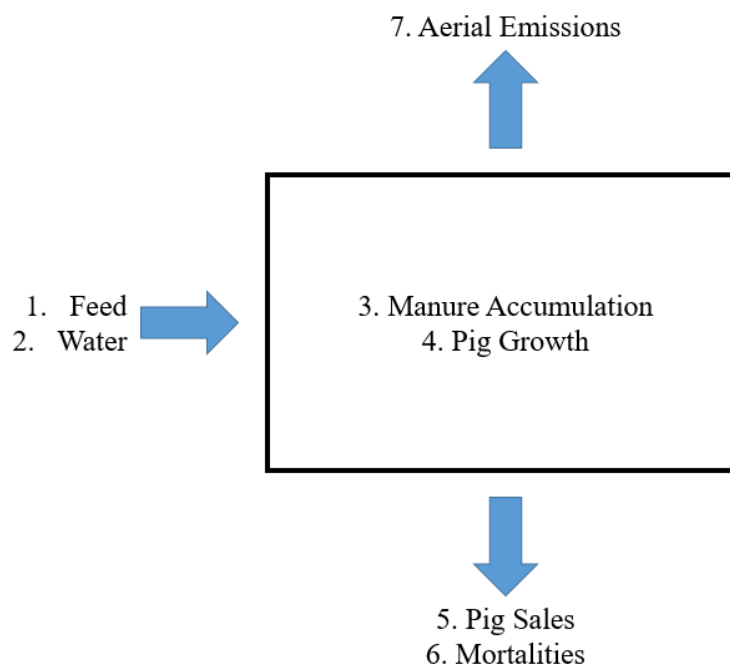


Figure 3.1 Depiction of mass balance principles used in this study.

3.3.3.1 Conventional Method

The conventional method used equations 3.1 and 3.2 to calculate the N and VS emissions for each sampling period. Balance variables used in the conventional mass balance are shown in Table 3.1.

Table 3.1 Mass balance components.

Balance Variable	Variable Name	Collection Method
1	Feed	Data from producers
2	Water	Water meter readings
3	Manure Accumulation	Stored manure depth
4	Pig Growth	Data from producers
5	Pig Sales	Data from producers

6	Mortalities	Data from producers
7	Aerial Emissions	Estimated via mass balances

$$N_1 + N_2 - N_3 - N_4 - N_5 - N_6 = N_7 \quad (3.1)$$

$$VS_1 + VS_2 - VS_3 - VS_4 - VS_5 - VS_6 = VS_7 \quad (3.2)$$

All N and VS components in equations 3.1 and 3.2 are expressed in mass per unit time.

This method used manure volume measurements to estimate manure accumulation.

3.3.3.2 Keener and Zhao (KZ) Method

The KZ method differed from the conventional method in the calculation of the manure accumulation. Rather than estimating VS and N from manure volume measurements, the KZ method uses ratios of N concentration of manure to ash concentration of manure ($R_{m,n}$) and VS concentration of manure to ash concentration of manure ($R_{m,a}$), along with remaining ash flows to estimate manure mass accumulation (Keener & Zhao, 2008). Equations 3.3 through 3.5 show manure accumulation for ash (A), N, and VS, respectively.

$$A_1 + A_2 - A_4 - A_5 - A_6 = A_3 \quad (3.3)$$

$$N_1 + N_2 - N_4 - N_5 - N_6 - R_{m,n}A_3 = N_7 \quad (3.4)$$

$$VS_1 + VS_2 - VS_4 - VS_5 - VS_6 - R_{m,a}A_3 = VS_7 \quad (3.5)$$

All A, N and VS components in equations 3.3 to 3.5 are expressed in mass per unit time.

Subscripts for equations 3.3 through 3.5 are defined in Table 3.1.

3.3.3.3 De Boer and Wiersma (DBW) Method

The DBW method applied a correction factor to all input, output, and storage streams, based on the mass balance of an inert component (De Boer & Wiersma, 2021). In this study, ash was used as the inert component. Due to measurement and sampling uncertainties of many balance variables, the sum of ash inputs did not equal the sum of ash outputs and storages. The percent of unaccounted-for ash was used to determine the correction factor applied to balance variables. Correction factors were used to equally redistribute the mass of unaccounted-for ash in the original balance. For example, if the unaccounted-for ash value was 20%, meaning the mass of input ash was 20% greater than the sum of output and storage ash, the mass of the inputs streams was reduced by 10%, and the mass of output and storage streams was increased by 10%. Equations 3.1 and 3.2 were used to estimate N and VS emissions using the adjusted balance streams.

3.3.4 Model Comparison Methods

After estimating CH₄ and NH₃ emissions for each sampling period using the three balance methods, several emission models were used for comparison of values. The IPCC methane emission estimation model was used for comparison to CH₄ emissions estimated through each balance approach (IPCC et al., 2019). Methane estimates for both Tier I and Tier II IPCC models were calculated, using both default literature input values and experimental input values for each sampling period. Figure 3.2 describes each iteration of the IPCC model, displaying the changes in input data from one iteration to the next. Input variables labeled as “sampled” indicate data gathered from the mass balances were used as

an input; input variables labeled as “book value” indicate input values came from literature values.

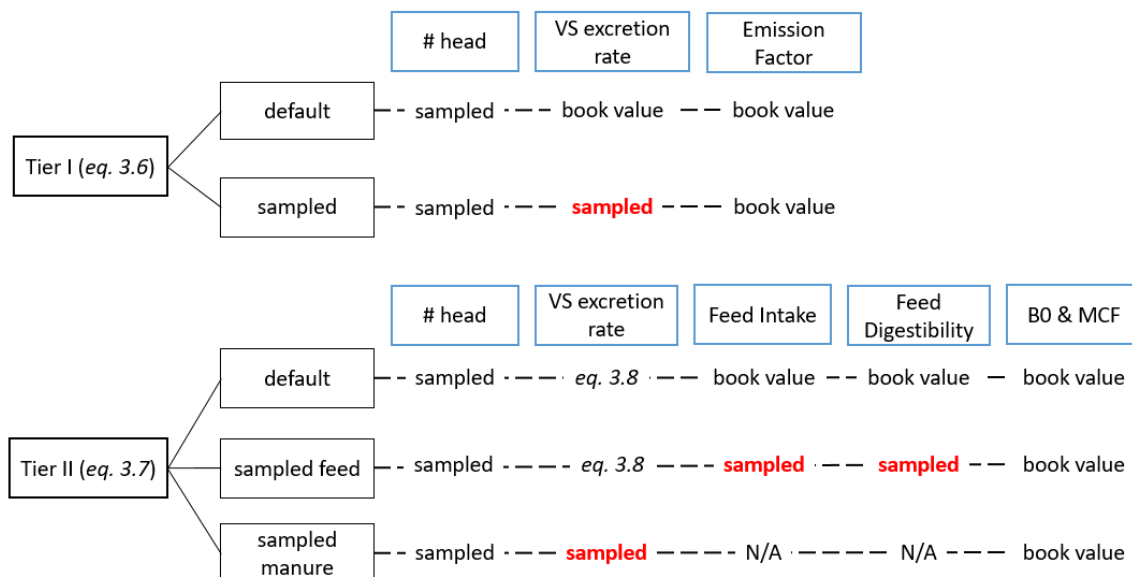


Figure 3.2 Flow chart of input values for each IPCC model iteration. Each iteration is labeled on the left in black boxes, and each input variable is labeled in blue boxes. Changes from default methods are denoted with red text.

Tier I emission estimates were calculated using equation 3.6:

$$CH_4 = P \times VS \times EF \quad (3.6)$$

where CH_4 is estimated methane emissions, P is number of head, VS is VS excretion rate, and EF is the emission factor.

Tier II emission estimates were calculated using equation 3.7:

$$CH_4 = P \times VS \times B_0 \times 0.67 \times \frac{MCF}{100} \quad (3.7)$$

where B_0 is the maximum methane producing capacity for manure produced, 0.67 is a conversion factor, and MCF is the methane conversion factor for the specified manure management system.

For Tier II default and sampled feed, equation 3.8 was used to calculate VS excretion rate:

$$VS = F_{DM} \times FI \times (1 - F_{DMD}) \quad (3.8)$$

where VS [$\text{kg d}^{-1}\text{a}^{-1}$] is VS excretion rate, F_{DM} [g/g] is dry matter content of feed, FI [$\text{kg d}^{-1}\text{a}^{-1}$] is feed intake, and F_{DMD} [%] is feed digestibility.

Ammonia emission estimations for each balance approach were compared to two models: the University of Nebraska – Lincoln (UNL) ammonia emission estimator worksheet (Koelsch & Stowell, 2005) and the draft EPA ammonia inventory model (U.S. EPA, 2020). The UNL ammonia emission estimator worksheet used estimated percent ammonia loss from animal housing and storage systems (from literature values), unit ammonia loss per animal (from literature values), and number of head, to calculate total ammonia losses. The EPA model used equation 3.9 to estimate ammonia emissions:

$$\ln(NH_3) = 1.3424 + 0.0091 \times T + 0.0085 \times LAM \quad (3.9)$$

where NH_3 is estimated ammonia emissions, T is ambient temperature, and LAM is live animal mass. It is important to note that this model was created specifically to estimate emissions from grow-finish operations, but it was still used as a comparison for site S1, a wean-finish operation.

3.4 Results and Discussion

3.4.1 Mass Distribution

Figure 3.3 shows the mass flow distribution between all balance variables for the 2023 sampling period at site S1. Water was excluded from this distribution as the mass of VS, N, and ash contributed to the system through water intake was considered negligible relative to other balance variables. Input variables are represented by positive values, while output and storage variables are represented by negative values. Figure 3.3 displays manure production as the most dominant variable in total mass distribution in all balance approaches, followed by feed intake. Figure 3.3 also displays graphically the mass flow adjustments made in both the KZ and DBW approaches. The KZ approach adjusts total manure mass while keeping the rest of the balance variables equal to the conventional approach; conversely, the DBW approach adjusts all balance variables from the conventional mass flows.

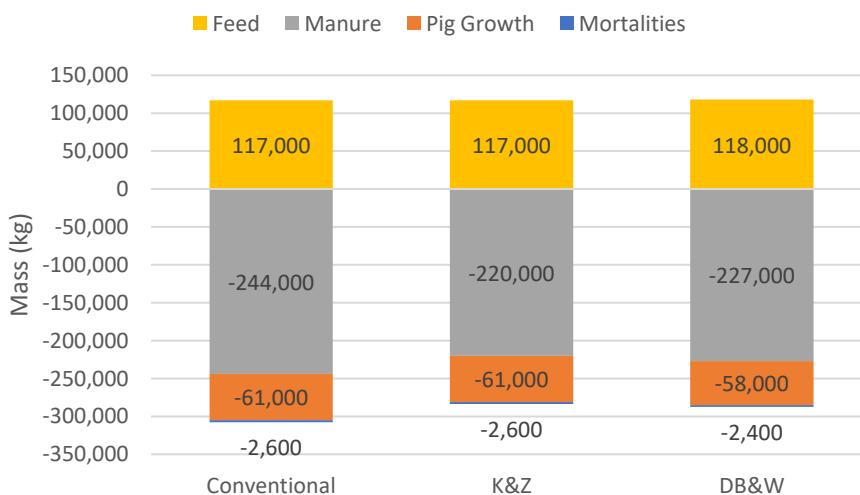


Figure 3.3 Total mass flow distribution measured in the 2023 sampling period of S1.

Table 3.2 shows the average measured concentrations of total solids, ash, VS, and N for the 2023 sampling period of S1, as well as typical concentration values found in the literature. Similar measured values were seen in the 2022 sampling period of S1, the 2022 sampling period of S2, and the 2023 sampling period of S2.

Table 3.2 Average measured and literature composition values for the 2023 sampling period of S1.

	Total Solids (%wb)		Ash (%wb)		Volatile Solids (%wb)		Nitrogen – TKN (%wb)	
	Measured	Book Value	Measured	Book Value	Measured	Book Value	Measured	Book Value
Feed	86.52	88.00 ¹	3.64	17.60 ^{1,a}	82.87	70.40 ^{1,a}	2.78	2.52 ¹
Manure	4.74	10.00 ^{1,b}	1.48	1.96 ^{1,b}	3.26	8.04 ^{1,b}	0.59	0.60 ²
Animal	-	27.69 ³	-	1.37 ²	-	26.32 ²	-	3.60 ²

Mass flow values as presented in figure 3.3 were multiplied by assumed concentrations of VS, N, and ash (table 3.2) for each balance variable. Figures 3.4 and 3.5 show the distribution of VS and N mass, respectively, for the 2023 sampling period at site S1. Mass distributions for the 2022 sampling period of S1 and the 2022 sampling period of S2 followed similar trends as seen in figures 3.4 and 3.5.

¹ (American Society of Agricultural and Biological Engineering, 2019)

² (Lorimor et al., 2004)

³ (Okrouhlá, et al., 2006)

^a based on feed digestibility

^b value as excreted

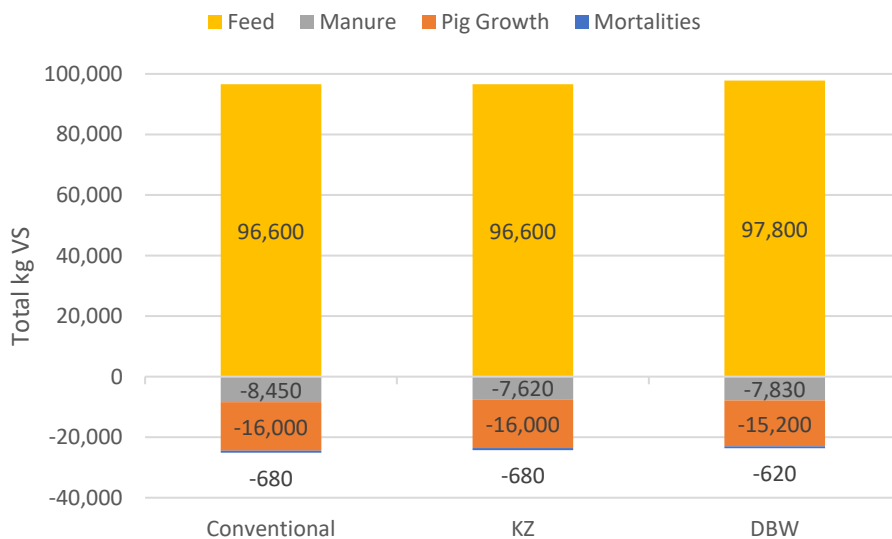


Figure 3.4 Mass distribution of total VS measured in the 2023 sampling period of S1.

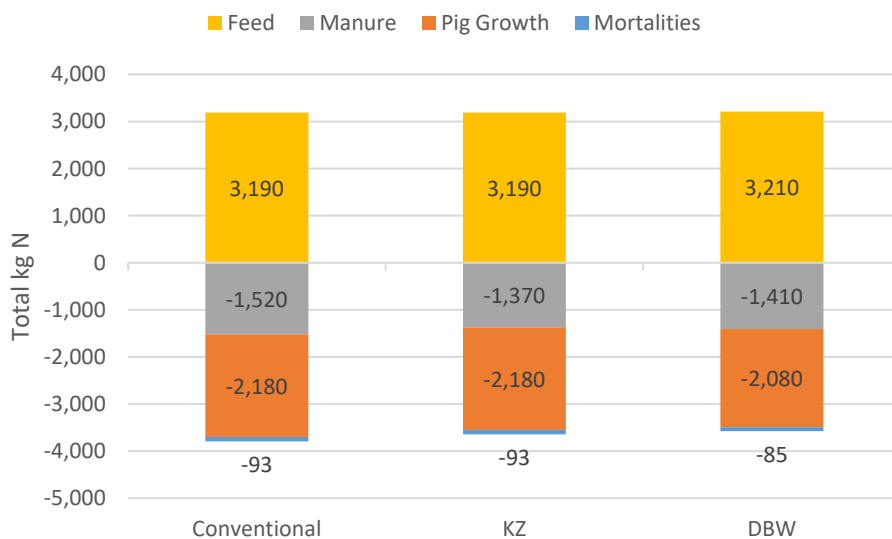


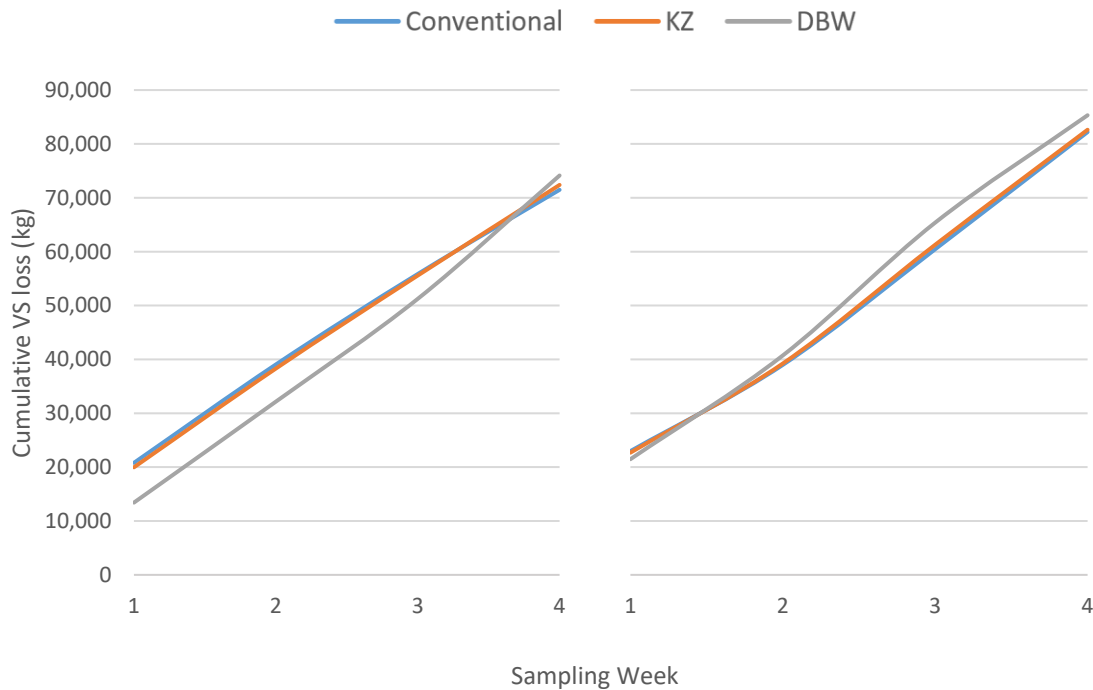
Figure 3.5 Mass distribution of total N measured in the 2023 sampling period for S1.

Figure 3.4 shows feed as the dominant source of VS, since there is such a high percentage of digestible material in growing pig feed. Accurate estimation of feed intake is crucial for an accurate VS mass balance. Figure 3.5 shows feed, manure, and pig growth

all as influential sources of N, making accurate estimation of manure production and animal growth crucial along with feed intake for an accurate N mass balance.

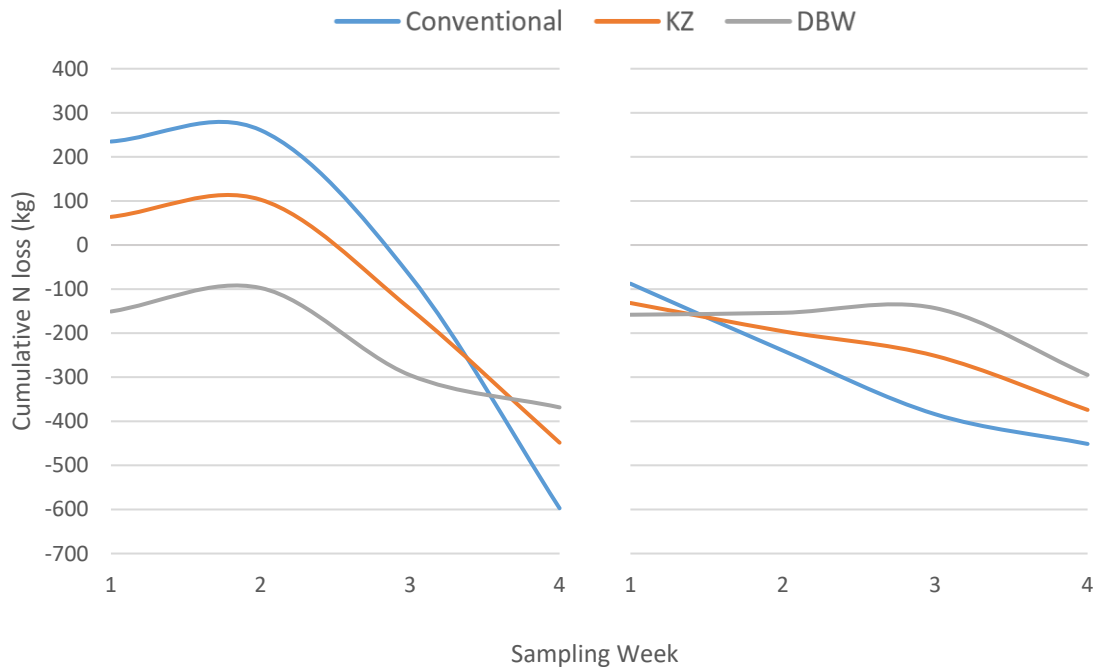
3.4.2 Cumulative VS and N losses

Each of the three balance approaches were used to find weekly and cumulative VS and N losses from each sampling period. Figure 3.6 shows the cumulative losses of VS for the 2023 sampling period of S1 and the 2022 sampling period of S2. Cumulative VS losses follow the expected trend, a linear increase in cumulative losses, signifying relatively similar losses each sampling week. Similar trends were seen in the other two sampling periods. There were little differences between each of the balance approaches. The KZ approach followed almost identical to the conventional approach, as only manure production is being adjusted. As seen in figure 3.4, manure production does not make up a significant portion of VS mass in the balance, so the KZ approach adjustment does not make significant changes to cumulative VS loss. The DBW approach made larger adjustments, since it evenly adjusts all input, output, and storage flows. Even with these larger adjustments, the DBW approach still follows closely to the conventional and KZ approach.



(a) (b)
Figure 3.6 Cumulative VS loss for (a) 2023 S1 sampling period and (b) 2022 S2 sampling period for each balance approach.

Figure 3.7 shows the cumulative losses of N for the 2023 sampling period of S1 and the 2022 sampling period of S2. Cumulative N losses were expected to follow a similar trend to the cumulative VS loss, a linear increase in cumulative N loss. However, cumulative N losses followed a non-linear decreasing trend, with negative loss values, signifying N gain in the system. This trend is also seen in the other two sampling periods. These negatives losses suggest potential sources of error in the sampling and analysis processes.



(a) (b)
Figure 3.7 Cumulative N loss for (a) 2023 S1 sampling period and (b) 2022 S2 sampling period for each balance approach.

As denoted in figure 3.5, feed intake, manure production, and animal growth were the most influential variables in the N balances. Since the cumulative VS loss trends, which are dominated by feed intake data, were consistent with expected results, manure production and animal growth estimates were the more likely sources of error. Manure production was estimated using a laser depth sensor, measuring from the top of the slatted floor to the manure surface. This depth measurement was recorded to the nearest inch. The depth was converted to total manure mass using the pit dimensions provided by the producers. Over a large surface area like those found in these manure pits, and with a sampling frequency of only one week, manure depth measurement to the nearest inch leaves significant room for error. In some instances, depending on animal size and activity,

stored manure depth does not change on the inch scale, and rounding to the nearest inch can significantly over- or underestimate total manure production. To improve manure production estimates, it is recommended to measure manure depth using a finer scale and sample less frequently than weekly.

Additional error is introduced with animal growth estimates. Average pig weights from the pigs housed during each sampling period were provided by the producers when available. The availability of these weights varied by site, with S1 providing more frequent averages and S2 providing just starting and ending average weights. Total animal mass was estimated using interpolated weights from those provided, which may not be fully representative of the actual animal growth during the sampling period.

Finally, there is potential for error in the assumed compositions for feed, manure, and the animal. As presented in table 3.2, measured VS and ash concentrations differed from literature values, with measured ash concentration considerably less than the literature value and measured VS concentration considerably greater than the literature value. Inaccuracies in these values could influence the overall VS and ash balances. Considerable uncertainty exists in the assumed body composition of the pigs as well. Very little data exists on the overall body composition of commercial pigs, and the values used (found in table 3.2) may not be completely representative of the turns of pigs during each sampling period.

3.4.3 Total CH₄ and NH₃ Emission Estimates

Total VS and N losses for each balance were converted to CH₄ and NH₃ emissions, respectively. Feed digestibility values of between 82 and 83% were used to assume the portion of VS losses attributing to CH₄ production, conversions from VS to CH₄ assumed 55% carbon content in VS. Conversions from N to NH₃ represent maximum potential NH₃ emissions, assuming 100% of N losses are attributed to NH₃ production. Figures 3.8 and 3.9 display total CH₄ and NH₃ emissions, respectively, for each balance approach.

Both figures 3.8 and 3.9 show differences in CH₄ and NH₃ estimates between sites and between sampling periods within the same site. According to previous research in the literature, CH₄ and NH₃ emissions can be influenced by both animal size and environmental conditions. The CH₄ emissions for S1 show significantly higher emissions for the 2022 sampling period, which took place near the end of a turn of pigs, while the 2023 sampling period took place near the beginning of a turn of pigs.

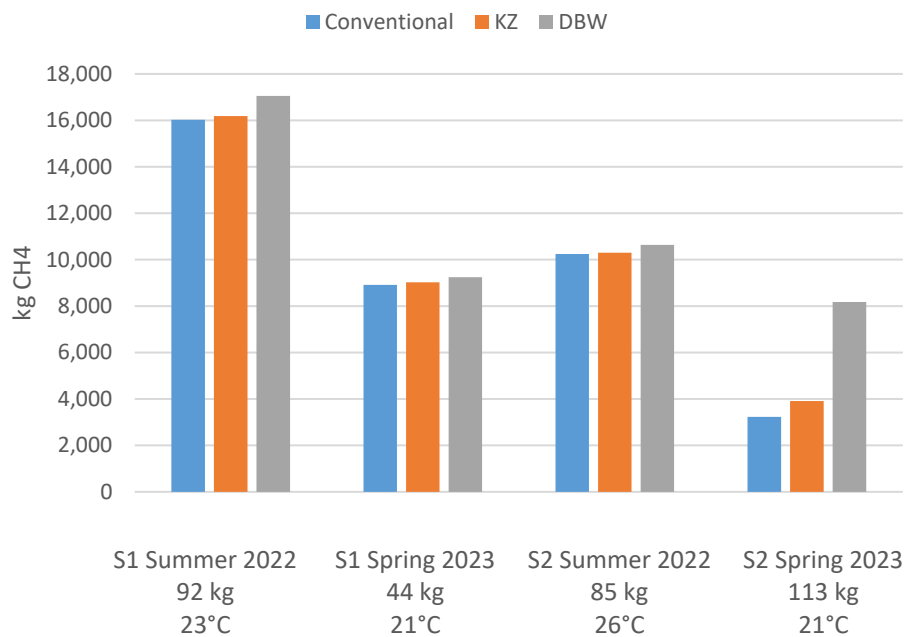


Figure 3.8 *CH₄ emission estimates for each sampling period and balance approach. Average live animal masses and barn temperatures are also included under each sampling period.*

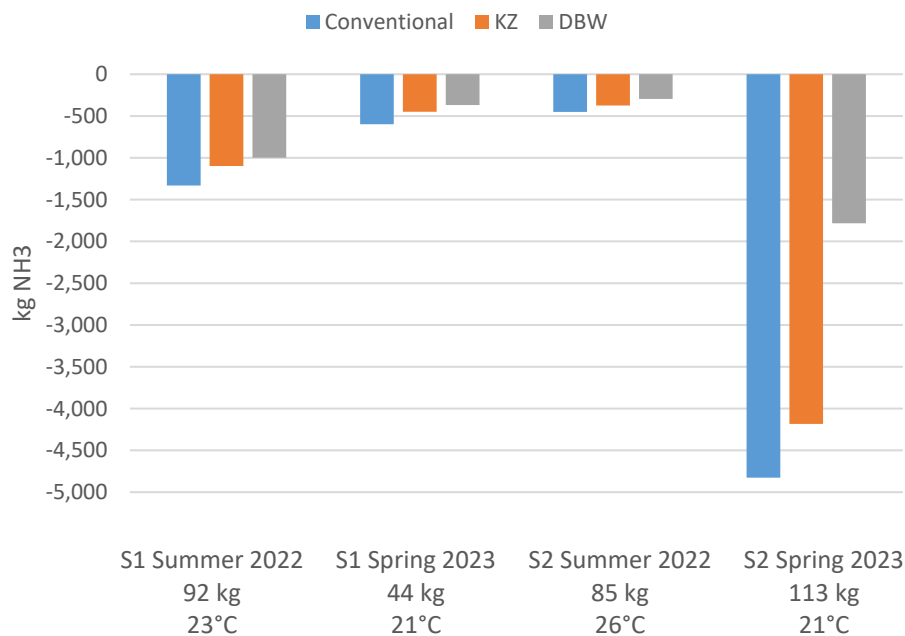


Figure 3.9 *NH₃ emission estimates for each sampling period and balance approach. Average live animal masses and barn temperatures are also included under each sampling period.*

The S2 Spring 2023 sampling period did not follow the same general trends as the other sampling periods in either CH₄ or NH₃ emissions. This sampling period took place at the end of a turn of pigs, and a majority of the pigs were sent to market over the course of sampling. This decrease in animal inventory not only skewed the mass distribution towards the outputs, but it also reduced weekly feed intake and manure production, creating lower CH₄ and more negative NH₃ emission estimates.

3.4.4 Generalized Linear Model for CH₄ Emission Estimates

Generalized linear models (GLM) for the total CH₄ emission estimate values for each balance approach were created using site, average live animal mass (LAM), average barn temperature (BT), and interactions as effect variables. The S2 Spring 2023 estimates were omitted from this analysis, as they were significantly influenced by the changing animal inventory. Values were compiled and run in JMP[®] Pro 16. Figures 3.10 through 3.12 plot CH₄ estimates for each balance along with estimates modeled through the corresponding GLM.

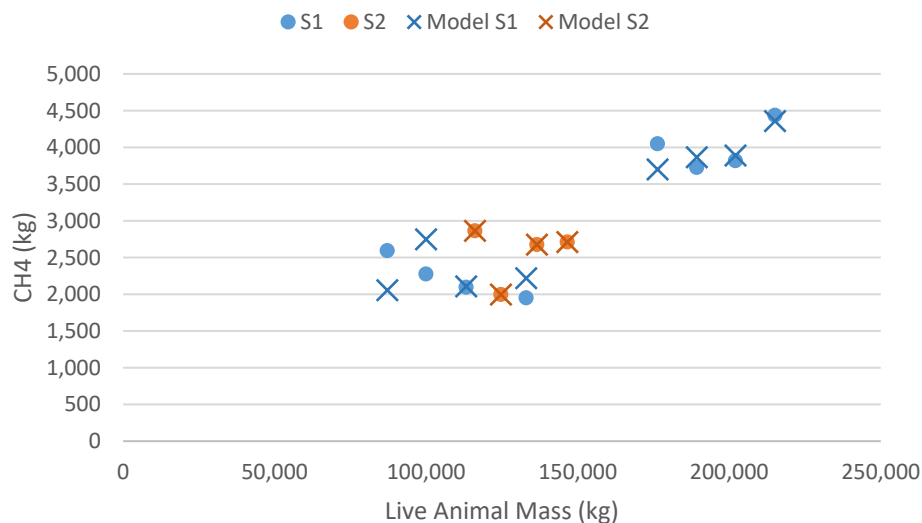


Figure 3.10 Conventional mass balance CH_4 estimates and GLM CH_4 estimates by average live animal mass. Values are categorized by site.

Live animal mass ($p = 0.0310$) and the interaction between LAM, BT, and site ($p = 0.0395$) both significantly influenced CH_4 emission estimates for the conventional mass balance. As seen in figure 3.10, as LAM increased, CH_4 emissions increased. The interaction is likely also statistically significant because of the higher average barn temperature in the 2022 sampling for S2 (26°C) compared to the temperatures in both S1 sampling periods (23°C and 21°C).

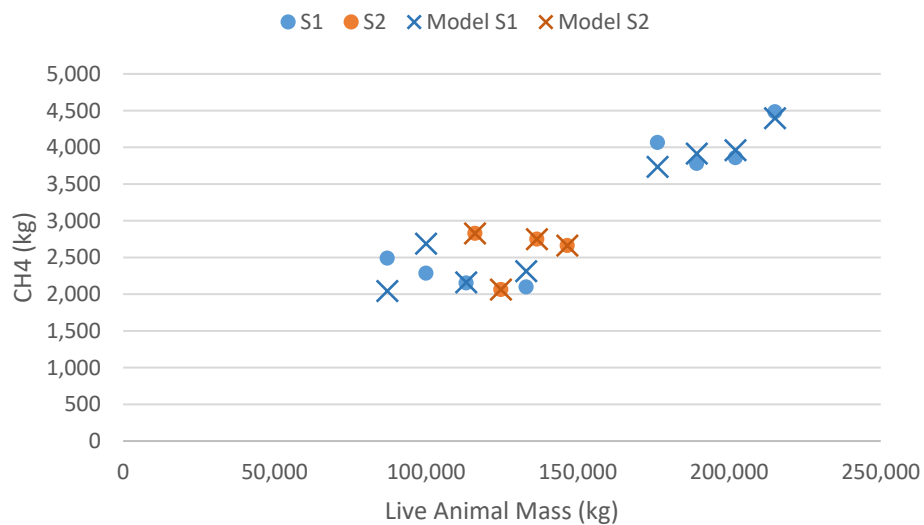


Figure 3.11 KZ mass balance CH₄ estimates and GLM CH₄ estimates by average live animal mass. Values are categorized by site.

Live animal mass ($p = 0.0161$) and all of its interactions significantly influenced CH₄ emission estimates for the KZ balance approach. Similar to the conventional balance GLM, this is likely due to varying temperatures between sites and sampling periods. In the KZ approach, CH₄ emissions again increase as LAM increases.

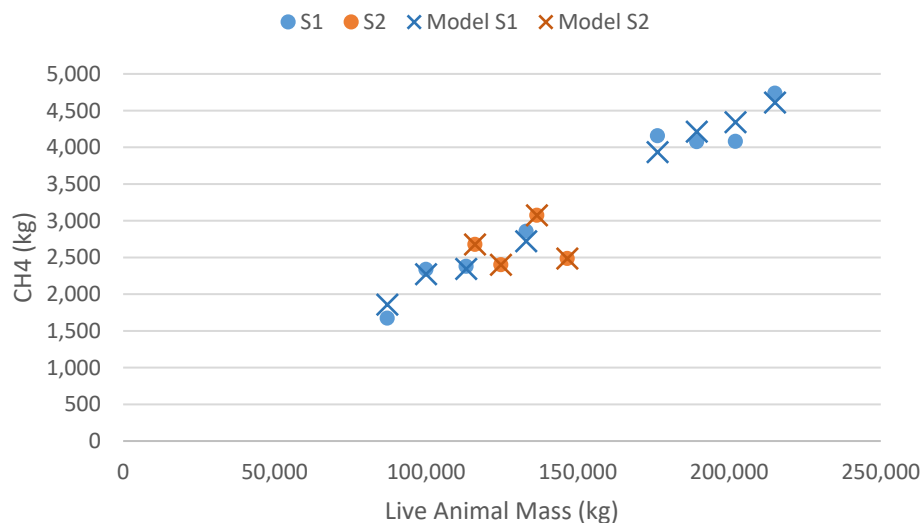


Figure 3.12 DBW mass balance CH_4 estimates and GLM CH_4 estimates by average live animal mass. Values are categorized by site.

All effects including site ($p = 0.0035$), LAM ($p = 0.0014$), BT ($p = 0.0012$) and all interactions between them significantly influenced CH_4 emission estimates for the DBW balance approach. Figure 3.13 plots CH_4 emission estimates against average barn temperature. There is a slight trend of increasing CH_4 emissions as BT increases. Figure 3.13 also exemplifies the differences between S1 and S2, where S2 is tied to higher barn temperatures.

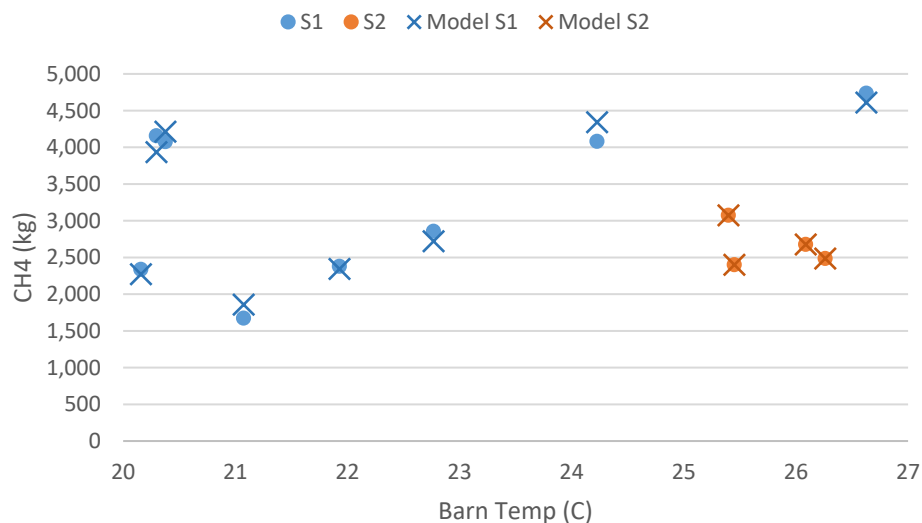


Figure 3.13 DBW mass balance CH_4 estimates and GLM CH_4 estimates by average barn temperature. Values are categorized by site.

For all mass balance approaches, LAM consistently influenced CH_4 emission estimates, with increasing LAM leading to increasing emissions. This relationship is consistent with those in the literature (Christensen & Thorbek, 1987; Noblet et al., 1989; Noblet & Shi, 1994). Additionally, the literature suggests that CH_4 generation in deep-pit manure storages favor higher manure temperatures, which barn temperature can influence (Philippe & Nicks, 2015).

3.4.5 Model Comparisons for CH_4 and NH_3

Methane emissions estimated through the three balance types were compared to the IPCC methane emission estimation model for all sampling periods (IPCC et al., 2019). The differences between each iteration of the IPCC model are described in figure 3.2. Figure 3.14 displays all CH_4 emission estimates from both the balances and the models. Estimates from each model were adjusted to represent the same number of days passed in each

sampling period. All mass balance approaches estimated significantly greater CH₄ emissions than the models, suggesting there may be error in either the VS mass balances and/or the assumptions used to convert VS to CH₄. Within the IPCC models, Tier II models estimated higher CH₄ emission than Tier I, as Tier II takes into consideration feed digestibility.

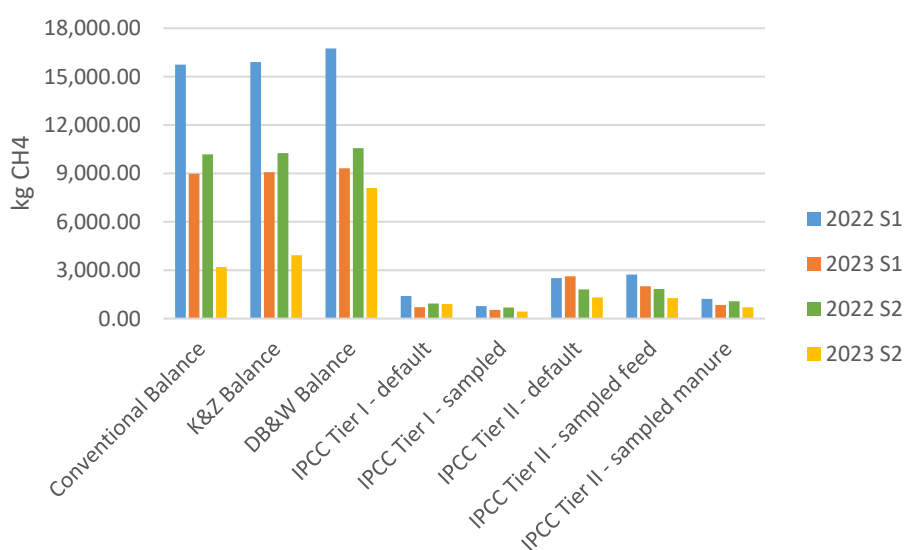


Figure 3.14 Total CH₄ emission estimates from each balance approach and model for all sampling periods.

Ammonia emissions estimated through the three balance types were compared to the UNL ammonia estimator tool and the EPA ammonia inventory model. Figure 3.15 displays all NH₃ emission estimates from both the balances and the models. Estimates from each model were adjusted to represent the same number of days passed in each sampling period. Estimates from the mass balances were not comparable to the model estimates, as they estimated negative emissions. There was also variation between the two models, with the UNL model estimating much higher NH₃ emissions than the EPA model. The UNL

model uses a constant value for assumed NH_3 excretion rate for a grow-finish pig, while the EPA model uses live animal mass and barn temperature as calculation factors.

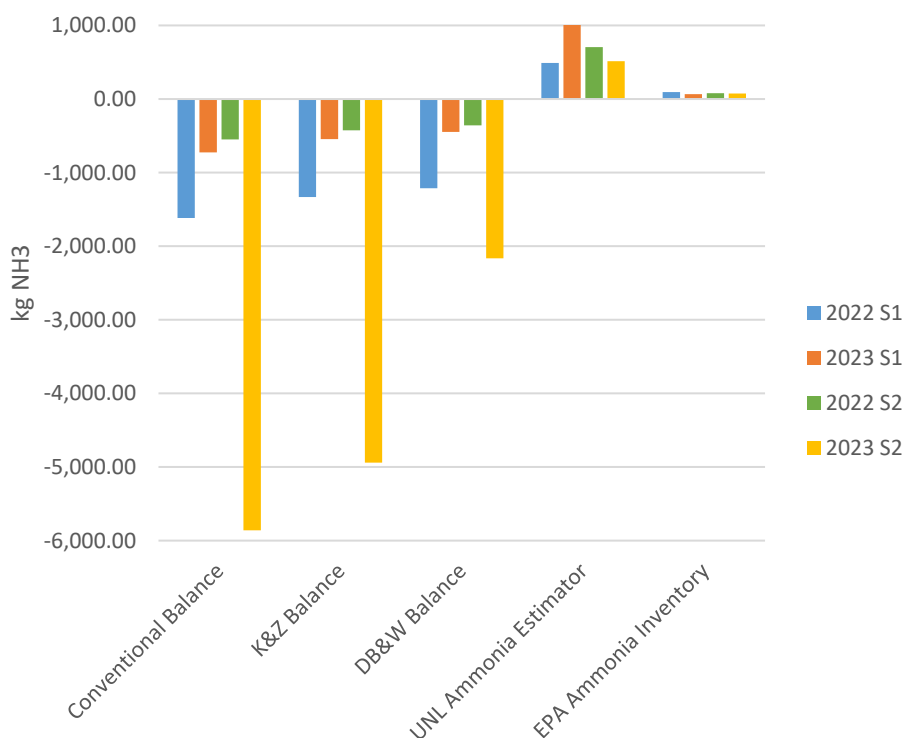


Figure 3.15 Total NH_3 emission estimates from each balance approach and model for all sampling periods.

Neither the CH_4 nor NH_3 emission estimates calculated via the mass balance approaches were similar to model values. This could signify error in the balance methods, or it could exemplify inaccuracies in the generalizations and assumptions made in modeling approaches. Regardless of how they compare to mass balance emission estimates, there are significant differences between each modeled emission estimate. Every model makes its own set of assumptions and has its own applicability to farm-level emission estimation. It is important to understand the assumptions and generalizations used

for each type of model to evaluate the credibility of its estimates. For CH₄, Andersen et al. (2015) did find agreement between IPCC estimates and a lab assay of deep pit swine manure; which means there are still options for farm-specific emission estimates for continued investigation.

3.5 Conclusion

Accurate estimates of manure production, feed intake, and animal growth are vital to reliable emission estimates using a mass balance approach. For mass balances using VS content, mass of feed intake is the most influential component of the balance; for mass balances using N content, masses of manure produced and animal growth are the most influential components. Along with accurate mass flows over time, accurate assumptions for balance variable compositions are also critical for accurate emission estimates; more work is needed to confirm the typical body composition for growing swine. Finally, a better understanding of swine feed digestibility and the portion of VS attributable to CH₄ emissions versus CO₂ emissions and/or animal growth/maintenance is necessary to improve the reliability of emission estimates.

Mass balance modifications like those presented in the KZ and DBW approaches can be advantageous if all assumptions are met. These approaches are dependent on the balance accuracy of a non-volatile component, which is also limited by the accuracy of tracking of all balance variables. Despite this, the use of these additional balances can aid in reducing larger measurement errors in the N and VS balance variables that influence the emission estimates.

In general, CH₄ emissions were influenced significantly by LAM, with emissions increasing with LAM. In some instances, CH₄ emissions were also significantly influenced by BT, again with emissions increasing with BT. These relationships are consistent with those presented in the literature. Using the methods presented in this research, emission estimates for CH₄ and NH₃ using a mass balance approach were not comparable to other modeled methods. This could lead to inaccuracies with the mass balance approach, or signify inaccuracies in the assumptions used for the model approaches.

3.6 Acknowledgements

Funding provided by the Rapid Agricultural Response Fund. We would also like to express our appreciation to farmer cooperators who assisted with data collection and provided their observations and insights throughout the sampling periods.

Chapter 4: Opportunities and Methods for Using Fluorescent Gel as a Proxy for Pathogen Transfer in Biosecurity Research⁴

4.1 Abstract

Glo Germ fluorescing material is a common tool for demonstration of contaminant transfer education and research, in and outside of agriculture. The objectives of this paper were to: (1) quantify relationships between gel area density (mass per unit area) on a surface and its luminance, and (2) identify factors important in measuring Glo Germ transfer from one surface to another. Varying densities of Glo Germ were applied to paper, plastic, and rubber surfaces; each combination replicated three times. Digital images collected over one hour were analyzed for luminance (average gray value per unit area) under ultraviolet light. Changes in mass were also measured. For the gel transfer objective, a fixed weight was placed over varying wet and dried fluorescent material densities on paper and plastic surfaces. Gel masses were weighed, and images of the surface and receptor were taken before and after transfer. Evaporation was significantly faster ($p = 0.0019$) from the paper surface compared to the plastic surface. Luminance did not change as gel evaporated from either surface. For each material, luminance initially increased with increasing density until a threshold, after which additional fluorescing gel density did not change luminance. The thresholds for paper, plastic, and rubber surfaces were 0.018, 0.014, and 0.041 g cm⁻²,

⁴ Published: Warmka, Anna, Erin L. Cortus, Kevin A. Janni, Abby Schuft, and Sally Noll. (2023) Opportunities and Methods for Using Fluorescent Gel as a Proxy for Pathogen Transfer in Biosecurity Research. *Journal of Agricultural Health and Safety*, 29(1), 57–70. <https://doi.org/10.13031/jash.15253>

respectively. Wet gel transfer test results suggest transfer is easier to quantify on the receptor as opposed to the source. Dried gel did not exhibit measurable transfer. This research found limitations in equating mass transfer and luminance, but luminance threshold values can inform maximum Glo Germ application for imaging purposes. These research results support continued research and outreach with fluorescent material to reduce and prevent the spread of disease or other harmful contaminants in food and animal production.

4.2 Introduction

In the livestock industry, disease outbreaks threaten the health and welfare of animal herds and flocks, agricultural workers, and the continuity of business for a region or country. A pathogen can be transmitted to a new host through direct contact with an infected agent or its secretions or indirect contact via a fomite contaminated with or by an infected agent (Martin, 2017). Many pathogens can spread through contact transmission, including Hepatitis A and B in humans (Davis et al., 1989; Nelson et al., 2020), Porcine Epidemic Diarrhea virus (Jung et al., 2020), the Porcine Reproductive and Respiratory Syndrome Virus (PRRSV) in swine (Dee et al., 2002), and Highly Pathogenic Avian Influenza among poultry (van der Goot et al., 2003). The focus is on intraspecies transmission, but there are zoonotic pathogens that transfer from animals to humans and vice versa (i.e., Dale & Brown, 2013; Peiris et al., 2007). On farms, notable mechanical transmission pathways are animal-to-animal contact, shared equipment uses, human habits and traffic patterns, and movement of live animals and mortalities (CFSPH, ISU, 2013;

USDA, APHIS, 2017). While the risk of infection depends on pathogen characteristics, dose, host susceptibility, and other factors, contact characteristics impact transmission rates for multiple pathogens.

Biosecurity is the suite of steps taken to reduce and prevent the spread of disease. In the absence of a specific disease outbreak or for the protection of the affected industry, models or proxies enable demonstration and quantification of transmission and exposure risks. Dee et al. (2002) demonstrated potentially significant modes of mechanical transmission of a field strain of PRRSV inoculated into carriers like snow and water by replicating common on-farm human behaviors within a field-scale model of a farm. Where they exist, modified live vaccines facilitate viral transfer rate measurements in place of viral strains (e.g. Dee et al., 2006). In the agricultural food production sector, Fenske et al. (2002) used the fluorescent tracer Calcofluor RWP to investigate the performance of chemical protective clothing as a method of exposure mitigation to pesticide application.

Another fluorescing product has several applications in agricultural and industrial research settings. Glo Germ (Glo Germ Co., Moab, UT) is an ultraviolet (UV) fluorescent product available in powder, gel, or aerosol form, and marketed to demonstrate contamination. Maitland et al. (2013) examined cross-contamination at a mock retail deli market, wherein a trained sensory panel ranked fluorescent gel presence in UV light pictures based on coverage and intensity. Conover and Gibson (2017) compared the effectiveness of foaming versus gel-based soap during handwashing. The metric for comparison was the absorbance of 370 nm light by any residual fluorescent compound in

a pooled sample of swabs extracted in ethanol. Call et al. (2017) investigated hazardous drug (HD) preparation and handling methods by simulating HD spread onto downstream surfaces using powdered fluorescent powder placed on exterior vial surfaces. They quantified spread based on the number of fluoresced pixels in vial images collected before and after handling. Anderson et al. (2018) used fluorescent powder to compare the effectiveness of showers and bench entry (physical barrier) protocols to no bench (no physical barrier) entries in commercial swine facilities. Barn workers picked up fluorescent powder from the floor surface in a barn entryway, and researchers used a grid system and the presence/absence of fluorescence to quantify contamination post entry protocol.

These previous studies demonstrated creative approaches to measure pathogen (or other harmful substance) transfer. The four Glo Germ studies accommodated the potential variability in fluorescent material application, transfer, and detection. The methods generated quantitative data to facilitate treatment comparisons; however, there is a lack of information regarding the potential to quantify actual mass transfer from the fluorescent substance. For example, hypothetically, if the contaminant concentration on a surface is known and the mass transfer of surficial material is available, the contact transmission rate can be quantified and compared to other transmission pathways like those via air. Halvorson and Hueston (2006) use the (log) mass of the contaminant and the percent available for transmission in the calculation of a pathogen exposure risk index in biosecurity programming. Contact surfaces vary, but the mass transfer is theoretically very minute and difficult to measure in field-scale situations. Thus, this research set out to

answer the question of whether fluorescing material traits relate to mass and subsequent mass transfer between two surfaces. The objectives of this study were to: (1) quantify the relationship between the area density (mass per unit area) of Glo Germ gel applied to a surface and its resulting luminance and determine whether the relationship depended on time and surface type; and (2) identify important factors affecting the ability to measure Glo Germ gel transfer from an application surface to a receptor. This study considered the traits of Glo Germ gel specifically and recognizes that the product is also available in powder and aerosol formats. Understanding fluorescent material traits supports future research and outreach methods for assessing contact transmission pathways and, ultimately, protecting humans and animals in food and livestock production.

4.3 Materials and Methods

Each experiment required fluorescent material, an initial application surface, an ultraviolet light source, background light conditioning, a camera, and image processing software. Glo Germ UV fluorescent gel (Glo Germ Co., Moab, UT) was used in all tests. A UV flashlight (UVL 1006, Glo Germ Co., Moab, UT) illuminated the Glo Germ. A custom-built curtained table (20 x 20 x 20 cm; fig. A2 in appendix) eliminated surrounding light exposure, which preliminary tests deemed an important variable for image analysis. All images were taken using a Digital Single Lens Reflex (DSLR) camera (Canon EOS Rebel SL1, Canon U.S.A. Inc., Melville, NY) with camera settings detailed in table A1 (located in the appendix). This camera was chosen to maintain consistency within the

laboratory (versus, i.e., multiple, personal cell phone cameras) while providing high-quality images.

ImageJ, an image processing and analysis software package, was used to quantify both fluorescent luminance and the area containing fluoresced pixels (Schindelin et al., 2012). Fluorescent luminance is a measurement that quantifies how much light is reflected off a surface. After importing an image file into ImageJ, the image was converted to an 8-bit grayscale image, assigning an intensity number (or “gray value”) between 0 and 255 to each pixel to define its brightness. On this scale, 0 equated to a pure black pixel, and 255 was a pure white pixel. To aid in analysis, a threshold was set to select only pixels above a specified gray value (155) to separate the Glo Germ gel area from the rest of the image. After the gel pixels were isolated, the area and mean gray value (MGV) were measured for both the fluoresced area and the surrounding image area. MGV is a luminance measurement found by taking an average of gray values for every selected pixel and outputting a single number between 0 and 255. The luminance density (mass per unit area) of the fluoresced area of an image could then be found by dividing the MGV by the image area, in units of cm^{-2} . Example images associated with the various steps are available in figure A3 (located in the appendix).

Three different application surfaces were used in this study. They were:

- Paper (sections of blank, white, continuous form paper);
- Plastic (sections of white polystyrene antistatic weighing dishes); and
- Rubber (sections of blue nitrile powder-free disposable gloves).

These three application surfaces were chosen because of their availability. They also represent potential transfer surfaces related to humans found in a livestock barn environment (i.e., record sheets, plastic markers, and gloves).

4.3.1 Test Series 1 Mass over Time

The first experiment evaluated two gel masses (0.5 and 1.0 g), two circular surface diameters (2 and 6 cm), and two surfaces (paper and plastic) in a factorial design (eight combinations) replicated three times ($n = 24$) to measure changes in mass (i.e., evaporation) of Glo Germ gel up to 60 minutes post application. All experimental units were prepared by drawing the appropriate circle size (i.e., 2 and 6 cm) in the center of the surface and labeling by surface type, circle diameter, and gel mass. Initial surface masses were recorded, and the desired gel mass was squeezed directly from its tube-shaped container and spread evenly across the circular area with a small, flat spatula while the mass was monitored on the precision scale. All application masses were measured on a precision balance with an uncertainty of ± 0.02 g (PGW 2502i, Adam Equipment Inc., Oxford, CT), allowing ten seconds to equilibrate for each mass reading. Experimental unit masses were recorded every two minutes for the first ten minutes, then every ten minutes for the remaining 50 minutes. Gel masses were found by subtracting initial surface masses from each experimental unit mass.

The average evaporation rates for each treatment combination over the hour-long test were compiled into JMP Pro 14® (SAS Institute Inc., Cary, NC) to run a mixed model

evaluating evaporation rates with material, circle diameter, initial mass, and interactions as fixed effects, a time block as a random effect, and a first-order autoregressive structure.

4.3.2 Test Series 2 Luminance over Time

Tests to determine whether gel evaporation changed the measured luminance density were done using the same eight combinations used in Test Series 1, replicated three times. After the desired gel mass was spread over the specified area and recorded, an image was taken of the surface. Experimental unit masses (i.e., the mass of both the surface and the gel) and images were recorded every ten minutes for one hour. All masses were measured on a precision balance (PGW 2502i), allowing ten seconds to equilibrate for each mass reading. All images were analyzed in ImageJ to measure the surface area (in cm^2) and MGV for both the gel and the surrounding area. The difference between those measurements was used to calculate corrected MGV per unit area (luminance density) for each image, and all values were compiled into JMP Pro 14® to run a mixed model evaluating luminance density with material, circle diameter, initial mass, and interactions as fixed effects, time block as a random effect, and an AR(1) repeated structure.

4.3.3 Test Series 3 Luminance Density Threshold

Preliminary experiments suggested there was a threshold beyond which additional gel mass per unit area would not increase luminance measurements. This test used ten gel densities between 0.01 and 0.1 g (in 0.01 g increments) spread over a 2 cm diameter circle on three source materials (paper, plastic, and rubber) in a factorial design (30 combinations), and three replicates of each combination. For the rubber source material,

two additional gel masses (0.2 and 0.5 g) were also used (32 total combinations) to further investigate whether previous observations of luminance density plateaus applied to greater masses. For each combination, the surfaces were prepared in the same manner as described in Test Series 2, and the appropriate gel mass was spread over the indicated area, measured on an electric microbalance with an uncertainty of ± 0.002 mg (Sartorius M5P, Sartorius AG, Bohemia, NY), allowing ten seconds to equilibrate for each mass reading. An image of each test surface was taken and analyzed in ImageJ to measure MG_V. Luminance densities were calculated by dividing the corrected MG_V by the area of a 2-cm diameter circle.

Luminance densities, with corresponding gel masses and source materials, were compiled into JMP® Pro 14 to run a fit least squares model analyzing luminance densities by mass, material, and interactions. Nonlinear curve fitting was also performed for each material using exponential curves (3P; eq. 4.1). To force the curves to intercept at approximately the origin, coordinates of (0, 0) were included in each replicate.

$$y = a + b * e^{c*mass} \quad (4.1)$$

where

y = luminance density, cm^{-2}

a, b, c = regression coefficients; mass = mass of gel, g

e = exponential constant

4.3.4 Test Series 4 Transferability of Wet Gel

Test Series 4 documented how the fluorescent gel transferred from one surface to another. Two initial gel masses (0.1 and 0.2 g), two circular surface diameters (2 and 4 cm), and two surfaces (paper and plastic) were used in a factorial design (eight combinations), replicated three times. The experimental units were prepared in the same manner as described in Test Series 1, and initial experimental unit masses and images were recorded. All masses were measured on an electronic microbalance for finer measurements (Sartorius M5P, Sartorius AG, Bohemia, NY).

To control the process of transferring from one surface (the source) to another (the receptor), a fixed, prepared transfer surface was used. The transfer surface was 218 g in weight, with nitrile material (a section of a glove) stretched across the flat, 2.735 cm diameter bottom surface and secured to the sides of the weight. The transfer surface was set on top of the test surface for 30 seconds. The final mass and luminance measurements of the test surface and the final luminance of the transfer surface followed the previous methods.

Each image was analyzed in ImageJ to measure area and MGv to calculate luminance density values. The differences between initial and final mass and initial and final luminance densities were calculated and compiled into JMP® Pro 14 to run a mixed model analyzing the effects of material, circle diameter, initial mass, and interactions on the changes in mass and luminance density.

To evaluate the luminance densities present on the receptor after transfer from each experimental unit (i.e., paper or plastic), all calculated luminance density values were compiled into JMP[®] Pro 14. A mixed model was run to analyze the effects of material, circle diameter, initial mass, and interactions on the change in luminance density, as well as the change in gel mass and the mass transferred onto the fixed weight.

4.3.5 Test Series 5 Transferability of Dried Gel

This test was like test 4, except that the fluorescent gel was allowed to dry before attempting transfer from the initial surface to the transfer surface. This test considered two gel masses (0.5 and 1.0 g), two circular surface diameters (2 and 4 cm), and two surfaces (paper and plastic) in a factorial design (eight combinations), replicated three times. The experimental units were prepared in the same manner as described in Test Series 1. All 24 surfaces were left to dry for two days at room temperature, with conditions consistent for all surfaces. Two days ensured enough time for surfaces to dry completely, based on observations from the researchers. After drying, the masses of each test surface were measured, and images of each were taken.

Each image was analyzed in ImageJ to measure area and MG. Those measurements were used to calculate luminance density values for each image. The same statistical analysis methods described in Test Series 4 were used to evaluate the change in luminance and mass at the source after transfer and to evaluate the luminance densities on the receptor.

4.4 Results

4.4.1 Test Series 1 Mass over Time

Circle diameter ($p < 0.0001$), surface material ($p < 0.0001$), and the interaction between circle diameter and surface material ($p = 0.0462$) significantly affected evaporation rates. There was no significant difference between 2 cm diameter circles on paper or plastic surfaces. The least squares mean estimate for paper with a diameter of 2 cm was $0.00153 \pm 0.00015 \text{ g min}^{-1}$, and it was $0.00137 \pm 0.00015 \text{ g min}^{-1}$ for plastic with a diameter of 2 cm. All other pairwise differences were significant (fig. 4.1). The evaporation rate increased overall for larger diameters. The estimate for paper with a diameter of 6 cm was $0.00467 \text{ g min}^{-1}$, which was significantly higher than $0.00405 \text{ g min}^{-1}$ for plastic with a diameter of 6 cm. This implies that gel spread over a larger surface area will have a higher evaporation rate regardless of the material, but there is more variability in evaporation rates between surface materials at larger surface areas.

Initial gel mass also significantly influenced evaporation rates ($p < 0.0001$). The least squares mean estimate for an initial mass of 0.5 g was $0.00261 \text{ g min}^{-1}$ and increased to $0.00320 \text{ g min}^{-1}$ for a greater initial mass of 1.0 g. This result was expected because it is assumed that experimental units with a higher initial mass density will have a higher evaporation rate.

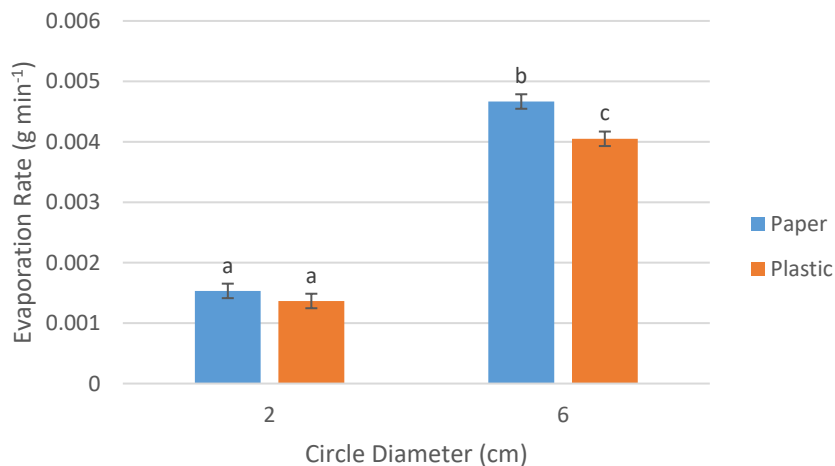


Figure 4.1 Least square mean estimates of average evaporation rates for interactions between material and circle diameter. Vertical standard error bars are 0.00012 g min⁻¹. Letters above bars denote significant differences.

4.4.2 Test Series 2 Luminance over Time

Luminance was significantly affected by surface material ($p = 0.0004$), circle diameter ($p < 0.0001$), and interactions between the surface material and circle diameter ($p = 0.0016$), but luminance was not affected by time ($p = 0.2883$) or initial mass ($p = 0.4788$). Figure 4.2 shows the difference in luminance between paper and plastic with a 2 cm diameter, while they do not differ at a 4 cm diameter. This suggests surface material is more influential on luminance for smaller coverage areas. Additionally, while luminance decreases as the circle diameter increases for each material, it does not decrease at the same rate; it decreases more rapidly on a paper surface than on a plastic surface. The reason for this difference is unknown, but it may come from the differences in reflectivity between paper and plastic. Since the paper has a lower reflectivity, measured luminance may be

more subject to change with coverage area because it is less influenced by background reflectance.

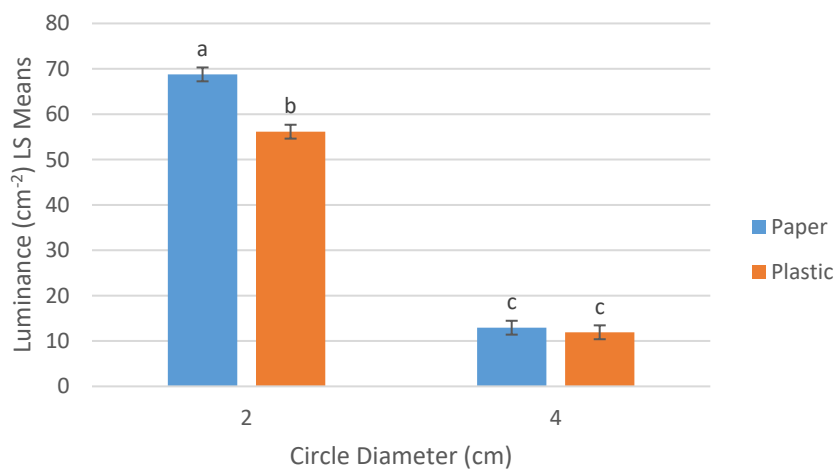


Figure 4.2 Least square mean estimates of luminance for interactions between material and circle diameter. Vertical standard error bars are 1.529 cm^{-2} . Letters above bars denote significant differences.

The insignificance of time on luminance suggests the fluorescent substance within the gel is not evaporating over time. Since luminance measurements are not sensitive to different masses (neither initially nor over time), the potential to estimate gel mass based exclusively on luminance is limited. Additionally, the insignificance of initial mass on luminance suggests there may be a luminance threshold, based on gel area density, after which the luminance no longer increases with the addition of more gel.

4.4.3 Test Series 3 Luminance Density Threshold

Luminance was significantly influenced by surface material ($p < 0.0001$) and mass ($p = 0.0103$), but not by interactions between the surface material and mass ($p = 0.1313$).

Figure 4.3 shows the average luminance density values as a function of average mass for each material; it also includes the exponential 3P curves fit for each material.

Figure 4.3 suggests there is a threshold after which adding more gel would not change the luminance density for a given mass density of Glo Germ. This maximum value is different for each surface material, most likely due to the different reflectivity of the materials, like that seen in test series 2. Since plastic reflects the greatest light, its background MGV is the largest, followed by rubber, then paper. This corresponds to paper having the largest corrected MGV, followed by rubber, and then plastic.

The asymptote parameter estimates represent the luminance density threshold for each surface material, after which increasing mass density would not increase luminance density. Although the maximum values differ between materials, the luminance density values reach that value at a consistently low gel mass. The luminance density reached within 0.1% of the asymptote value at 0.056 g of gel for paper, 0.043 g for plastic, and 0.130 g for rubber. Considering the 2 cm diameter circle area, this equates to mass densities of 0.018, 0.014, and 0.041 g cm⁻², respectively.

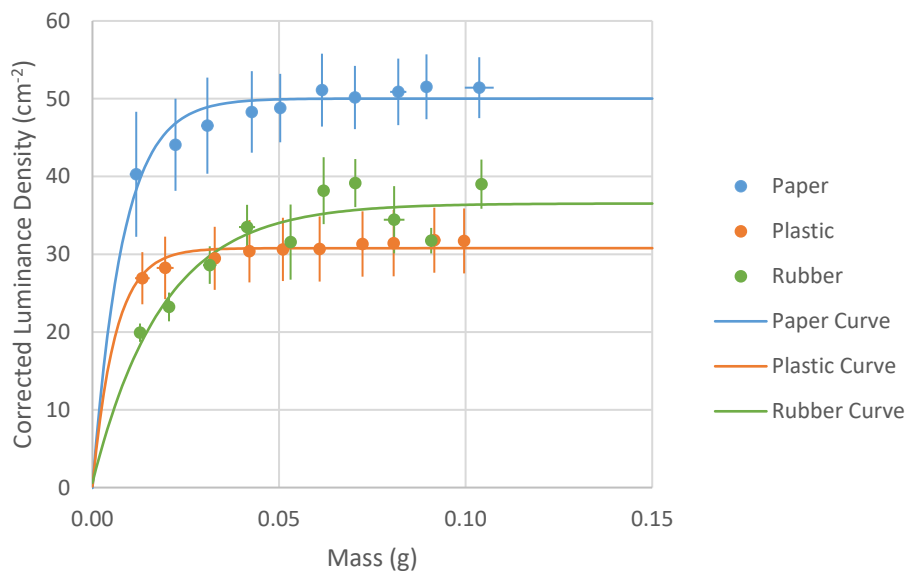


Figure 4.3 The average luminance density values versus mass for each material ($n=3$), along with the fitted curves for each material. Average corrected luminance densities of 38.4 cm^{-2} and 34.8 cm^{-2} for 0.2 g and 0.5 g , respectively for a rubber surface were excluded to highlight the results from 0 to 0.1 g . Horizontal and vertical bars indicate the standard error for each material and mass combination.

4.4.4 Test Series 4 Transferability of Wet Gel

Analyzing the changes in the source surface luminance before and after transfer found significance for the initial mass ($p = 0.0021$), circle diameter ($p < 0.0001$), and interactions between the two ($p = 0.0060$), while the material was insignificant ($p = 0.8450$). There was no significant difference with 4 cm diameter circles for the two initial masses. The change in luminance ranged from -0.1002 to 0.3642 cm^{-2} for 4 cm circles. Least square means estimates indicate that the luminance on the source surface did not change after mass transfer to the weight for a 4 cm circle diameter. This is likely because the diameter of the fixed weight was less than 4 cm and the mass densities in both cases (0.25 g cm^{-2} and 0.5 g cm^{-2}) were greater than the thresholds found for paper and plastic

surfaces in Test Series 3. A significant change in luminance was seen for the 2 cm circle diameter combinations, likely because the diameter of the fixed mass was greater than 2 cm, causing the final gel area on the source to increase. Since luminance is directly dependent on the coverage area, the increase in the area after the transfer caused the final luminance to decrease. All other pairwise differences were significant (fig. 4.4).

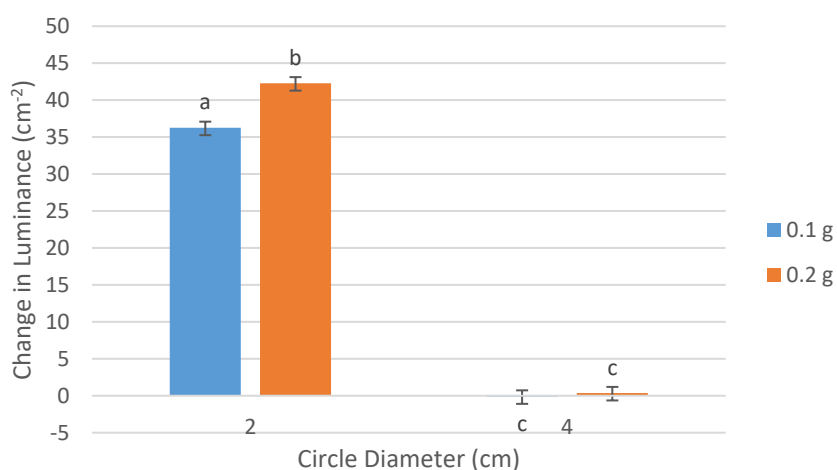


Figure 4.4 The change in luminance least square mean estimates for each initial mass and circle diameter combination. Vertical standard error bars are included, and letters above bars denote significant differences.

A mixed model to determine the significance of each factor and their interactions on the change in mass of the source surface found significance in material ($p < 0.0001$), initial mass ($p < 0.0001$), circle diameter ($p < 0.0001$), and the interactions between material and initial mass ($p = 0.0124$), material and circle diameter ($p = 0.0440$), and initial mass and circle diameter ($p = 0.0066$). Least square means estimates for material and circle diameter combinations showed no significant difference between Paper with a gel diameter

of 2 cm (0.0602 ± 0.0035 g) and Plastic with a gel diameter of 4 cm (0.0724 ± 0.0035 g).

All other pairwise differences were significantly different (fig. 4.5a).

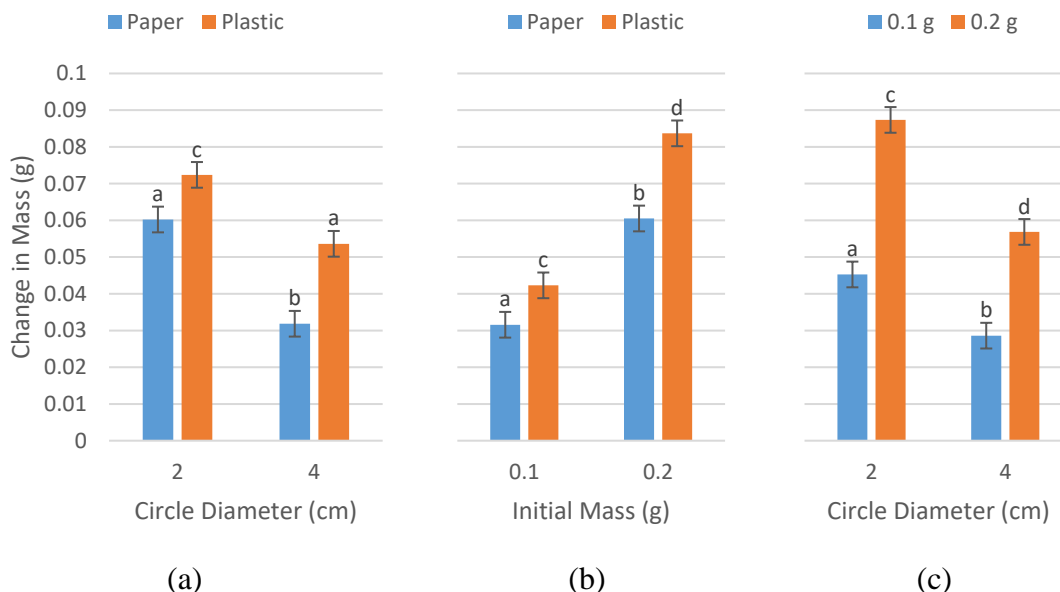


Figure 4.5 The least square mean estimates for mass loss from the source surface in wet gel transfer tests for combinations of material and circle diameter (a), material and initial mass (b), and initial mass and circle diameter (c). Vertical standard error bars are included, and letters above bars denote significant differences.

The results suggest combinations with a larger initial mass had a larger change in mass at the source, which was expected, but the source material influenced the degree of mass change (fig. 4.5b). In general, there is a greater change in mass for a plastic source surface when compared to paper, meaning the gel tends to transfer more easily off plastic compared to paper surfaces.

The significant interaction between initial mass and circle diameter shows that sources with a larger initial mass had a larger change in mass, but the degree of change was influenced by the area it was spread across (fig. 4.5c). Combinations with the 4 cm circle

diameter had a smaller change in mass than those with the 2 cm diameter circle, likely due to their gel area in relation to the receptor transfer area. The same gel mass spread across the 4 cm diameter circle created a thinner layer of gel than that found across the 2 cm diameter circle, so the receptor came into contact with less gel during transfer.

A mixed model to determine the significance of each factor and its interactions on the luminance transferred to the fixed weight found the source material to be significant ($p = 0.0303$). The least square mean for paper was $23.4 \pm 1.3 \text{ cm}^{-2}$, and it was $19.3 \pm 1.3 \text{ cm}^{-2}$ for plastic. This suggests the gel transfers off a paper surface more easily than a plastic surface, which is not consistent with the results from the changes in mass at the source. Overall, since there are so many factors influencing the changes in luminance and mass on the surface, namely the relative sizes of the source and receptor, it is preferable to focus results on changes in mass and luminance to the receptor as opposed to the source.

4.4.5 Test Series 5 Transferability of Dried Gel

Analyzing the change in luminance before and after the transfer of the sources with dried gel found no significant factors, indicating there was no significant transfer between the source and receptor. Observations during testing supported this conclusion, as the dried gel remained fixed to the initial surface with little to no visible transfer onto the fixed weight. A second mixed model to evaluate the change in mass at the source found material ($p < 0.0001$), initial mass ($p = 0.0015$), and circle diameter ($p = 0.0020$) significant, but all interactions were insignificant. Least square means estimates suggested plastic ($0.000946 \pm 0.000059 \text{ g}$) had a significantly larger change in mass when compared to paper (0.000373

± 0.000059 g), implying the dried gel sticks better to a paper surface versus plastic. Additionally, an initial mass of 1.0 g had a least square mean of 0.000848 ± 0.000059 g, while an initial mass of 0.5 g had a value of 0.000471 ± 0.000059 g, suggesting that a greater mass of dried gel transfers off a surface when the initial mass is greater. A circle diameter of 2 cm (0.000842 ± 0.000059 g) had a significantly greater change in mass than a circle of 4 cm (0.000477 ± 0.000059 g). This is likely because of the size of the transfer surface relative to the area of the source. Since the 2 cm source area is smaller than the transfer surface, there is more opportunity for the weight to fully stick to the dried gel, as opposed to the 4 cm source area, which is larger than the transfer surface.

A mixed model considering the significance of each factor and interactions on the luminance transferred to the fixed weight found material ($p = 0.0046$) and circle diameter ($p < 0.0001$) as significant factors. The least square means showed that transfer from a paper source ($14.8 \pm 0.6 \text{ cm}^{-2}$) was greater than that from a plastic source ($10.9 \pm 0.6 \text{ cm}^{-2}$). Although the least square means from the change in mass on the source would suggest the opposite would occur, this result exemplifies the difficulty present in relying on the change in the source gel mass or luminance as a way to quantify transfer. Additionally, the least square means showed that transfer from a 2 cm diameter circle ($20.1 \pm 0.6 \text{ cm}^{-2}$) was greater than from a 4 cm diameter circle ($5.61 \pm 0.63 \text{ cm}^{-2}$). This, again, is likely due to the relative sizes of the source areas compared to the transfer surface.

4.5 Discussion

This research demonstrated that evaporation affects scenarios when using gel as a proxy for contamination. Source material, surface area, and initial mass influence gel evaporation rates. Gel evaporation can change the gel's properties and performance, most notably its ability to simulate transfer from one surface to another. As the gel evaporates, the luminance does not change, suggesting it would be very difficult to accurately estimate mass transfer based solely on measured luminance. However, the lack of change in luminance with evaporation allows researchers to collect luminance measurements for a longer period of time in an experiment where demonstrating contamination is more important than mass transfer. If luminance is the measurement of choice, a longer stability period eases data collection in large spaces (i.e., barns), and over time. Fenske et al. (2002) and Anderson et al. (2018) comment on waiting periods or cleaning periods between trials necessary to eliminate residual tracer material between tests, with protocols dependent on the use scenario. The gel cannot be used to simulate contamination by transfer after it is dry because it tends to stick to its source material after it dries. If wet gel is used to simulate transfer, it is best to focus on quantifying gel transferred to the receptor rather than the difference before and after transfer from the source. Traits of other Glo Germ formats, like the dry powder, are likely less affected by evaporation over time for transfer tests. Evaporation must also be considered in outreach demonstration planning, considering the time between application to a surface and detection, and if a transfer is part of the demonstration.

In experimental research including mass transfer, it seems necessary to keep gel mass densities below threshold values to use luminance as an indicator of mass density. Since the mass density threshold is different for different materials, calibration must be done to determine the threshold for a specific material before beginning each experimental data collection. The procedure laid out in Test Series 3 provides a calibration method that can be used by researchers to fit the specific experimental designs, which include varying surface areas and materials. Other surfaces that could be explored to better represent the agricultural industry include various metals, different wooden surfaces, and glass. Since this series of tests was done at a lab scale, more research needs to be done to ensure the mass density thresholds persist for larger surface areas. More considerations when scaling up this procedure include guaranteeing a method of light control is in place and large enough for the test area and keeping all camera settings consistent across images. In mock or field-scale settings, several researchers comment that fluorescent material is more valuable as a qualitative tool than a quantitative tool for research, considering the variability in the test subjects and surfaces (Conover & Gibson, 2017; Harrison et al., 2022).

Any proxy has benefits and limitations in its representation of something else. This research furthers the understanding of where and how fluorescent gel material characteristics influence luminance and mass density measurements. Fluorescent substances continue to be a valuable tool in agriculture for investigating and demonstrating modes and rates of pathogen or contaminant transfer without having to inoculate surfaces

with these potentially harmful substances, using many creative methods described by previous researchers. Quantification data still seems limited to luminance, versus mass metrics, but this research provides guidance for dosing to ensure consistent luminance data.

4.6 Conclusion

A series of tests with Glo Germ gel identified opportunities and limitations for its use in research settings in the agricultural industry. Gel evaporated over time, causing the mass of Glo Germ on a surface to change. However, the luminance did not change during evaporation. There was a linear relationship between luminance and mass up to specific gel mass density values for paper, plastic, and rubber source materials (0.018, 0.014, and 0.041 g cm⁻², respectively). Beyond the mass density thresholds, the luminance no longer changed. The gel showed no significant transfer after being allowed to dry for two days on any surface, but there was a significant transfer when the gel was still wet. Quantifying the transfer of wet gel based on the changes to the source was influenced by several other factors, including the source material, initial gel mass, and the circle diameter size in relation to the receptor, suggesting focusing on quantifying the gel transferred is preferable to quantifying change in gel on the receptor. Glo Germ gel is a safer approach in agricultural settings to simulate surface transfer without having to use harmful substances like pathogens or chemicals. Surface transfer can be quantified to better understand areas of concern and the effectiveness of potential transfer reduction strategies.

4.7 Acknowledgements

Funding provided by the State of Minnesota Agricultural Research, Education, Extension and Technology Transfer program.

Chapter 5: General discussion

5.1 Overall Summary

In these two projects, methods were adapted and created to aid in research efforts towards increasing environmental and economical sustainability in livestock operations through the estimation of GHG production and quantification of biosecurity risk. These methods were evaluated via comparison to existing models and potential for application in on-farm research.

Chapter 3 estimated CH₄ and NH₃ emissions from Minnesota deep-pit swine barns using three mass balance variations for their precursors, VS and N, respectively. Insights on sampling methods and variations in emission estimates between barns, animal size, and environmental conditions were presented. Comparison of measured emission estimates to existing emission estimation models provided a better understanding of the uncertainties and assumptions using a mass balance approach.

Chapter 4 investigates characteristics of Glo Germ gel to identify opportunities and limitations for its use in livestock biosecurity research. A quantification method using the luminance and surface area of the gel was created, and important characteristics influencing this method were identified. Transfer from one surface to another was quantified, and factors affecting the ability to effectively quantify transfer were described in the analysis.

5.2 Limitations and Future Works

Chapter 2 described some criteria necessary for choosing an emission estimation approach, including measurement location, measurement frequency, and instrument sensitivity, chosen based on the research objectives. Proper choices for these parameters is necessary for reliable emission estimates that capture the spatial and temporal variations in emissions from a barn. When these criteria are met, limitations to the chosen estimation approach often stem from the sampling approach. Sampling limitations are often due to time and labor constraints, or lack of consistent, accurate data, as explained in chapter 3.

In chapter 3, sampling did not directly measure gas concentrations or airflow, so the accuracy of emission estimates were reliant solely on the accurate tracking of balance components, especially manure production, feed intake, and animal growth. Manure was sampled for this project; however, with such a large volume of manure stored at a time, obtaining a sample representative of the composition of the manure was difficult. Additionally, manure sampling frequency and depth measurement precision chosen created large potential for error in manure production estimates. Feed intake data accuracy varied between sites, but assumptions, estimations, and interpolations were used in all sampling periods. Several other assumptions regarding pig body composition, animal growth rates, and feed nutrient partitioning for metabolic processes were made for all sampling periods, which may not have been representative of these turns of pigs. Additional assumptions were made on the portions of VS and N attributing directly to CH₄ and NH₃ emissions, respectively, creating additional room for error.

Future research is still needed to understand the opportunity to apply a material mass balance approach to deep-pit swine farms for accurate emission estimation at the farm-level. Longer sampling periods with a lower sampling frequency are necessary to reduce the potential for error in manure production estimations; using more precise depth measurements will also aid in this effort. Comparison of emissions estimated via a mass balance to estimates from simultaneous aerial sampling at the same site also provide an opportunity to evaluate the accuracy of the mass balance method. Although comparison to model approaches allow for identification of uncertainties or inaccuracies in the balance approach, the models fail to represent all management characteristics of a specific operation and cannot account for spatial or temporal variabilities in emissions.

In chapter 4, the Glo Germ gel quantification method presented relies on a controlled environment for consistent luminance estimation. While controlling the environment in a small-scale, lab setting is fairly simple, applying this method to a livestock environment open up the opportunity for many more variable factors. Additionally, quantification is limited to measured luminance, versus mass metrics, and accurate quantification of surface transfer is limited to evaluating the receptor surface, versus evaluating the change in the source surface.

Future research is necessary to ensure luminance threshold values presented persist for larger surface areas, and to expand the surface types to include a better representation of the surfaces found in a livestock environment. There is also potential to expand this research to include trials representative of on-farm tasks that pose biosecurity risks and

quantify these risks with the use of the fluorescent gel. Development of techniques for controlling the light environment for a more expansive area will be crucial in creating a method for using fluorescent material as an accurate, quantitative method in field research.

5.3 Conclusions

Methods to create reliable estimation for gas emissions and biosecurity risk from livestock systems are crucial to address the concerns and priorities of different stakeholders. There are several strategies available for gas emission estimation, however it is important to choose the appropriate strategy based on the livestock environment of interest and research objectives. This work identified important measurement criteria to consider in developing a sampling plan and demonstrates the application and limitations of a mass balance approach in deep-pit manure storage systems. Improvements in sampling methods come with increasing complexity, which is not always feasible. While a mass balance approach includes its own set of limitations and assumptions, this work identifies areas for improvements in methods and analysis.

There is a lack of standard quantification methodology for fluorescent material use as a proxy for pathogen transfer, which is crucial for safe research of biosecurity risk and risk mitigation. This work identified the important factors in creating consistent quantification of a fluorescent gel at the lab scale. Expansion on this research is necessary to understand the feasibility for application to larger surface areas and field settings, however this work presents a quantification method for fluorescent gel on various surfaces.

Bibliography

- Aarnink, A. (1997). Ammonia emission from houses for growing pigs as affected by per design, indoor climate and behaviour. *Prof.Dr.Ir. L. Speelman, Prof.Dr.Ir. M.W.A. Verstegen (Supervisors), Dr.Ir. J.H.M. Metz (Co-Supervisor). Wageningen Agricultural University (1997) 175 Pp. ISBN: 90-5485-662-9.*
- Aarnink, A., & Elzing, A. (1998). Dynamic model for ammonia volatilization in housing with partially slatted floors, for fattening pigs. *Livestock Production Science*, 53(2), 153–169. [https://doi.org/10.1016/S0301-6226\(97\)00153-X](https://doi.org/10.1016/S0301-6226(97)00153-X)
- Aarnink, A., Keen, A., Metz, J., Speelman, L., & Verstegen, M. (1995). Ammonia Emission Patterns during the Growing Periods of Pigs Housed on Partially Slatted Floors. *Journal of Agricultural Engineering Research*, 62(2), 105–116. <https://doi.org/10.1006/jaer.1995.1069>
- Aarnink, A., & Wagemans, M. (1997). Ammonia volatilization and dust concentration as affected by ventilation systems in houses for fattening pigs. *Transactions of the ASAE (USA)*.
- Adams, H., Williams, A., Xu, C., Rauscher, S., Jiang, X., & McDowell, N. (2013). Empirical and process-based approaches to climate-induced forest mortality models. *Frontiers in Plant Science*, 4. <https://www.frontiersin.org/articles/10.3389/fpls.2013.00438>
- Ahring, B. K., Angelidaki, I., Conway Macario, E., Gavala, H. N., Hofman-Bang, J., Macario, A. J. L., Oude Elferink, S. J. W. H., Raskin, L., Stams, A. J. M., Westermann, P., & Zheng, D. (2003). *Biomethanation* (1st ed.). Springer. <https://doi.org/10.1007/3-540-45839-5>
- American Society of Agricultural and Biological Engineering. (2019). *ASAE D384.2 MAR2005 (R2019) Manure Production and Characteristics*. ASABE. <https://elibrary.asabe.org/abstract.asp?aid=32018&t=2>
- Amon, B., Kryvoruchko, V., Amon, T., & Zechmeister-Boltenstern, S. (2006). Methane, nitrous oxide and ammonia emissions during storage and after application of dairy cattle slurry and influence of slurry treatment. *Agriculture, Ecosystems and Environment*, 112(2–3), 153–162. Scopus. <https://doi.org/10.1016/j.agee.2005.08.030>
- Andersen, D. S., Van Weelden, M. B., Trabue, S. L., & Pepple, L. M. (2015). Lab-assay for estimating methane emissions from deep-pit swine manure storages. *Journal of Environmental Management*, 159, 18–26. <https://doi.org/10.1016/j.jenvman.2015.05.003>
- Anderson, A. V., Fitzgerald, C. J., Baker, K. L., Stika, R. A., Linhares, D. C. L., & Holtkamp, D. J. (2018). Comparison of shower-in and shower-in plus bench entry protocols for prevention of environmental contamination due to personnel entry in a commercial swine facility. *Journal of Swine Health and Production*, 10.
- AOAC. (1995). Protein (Crude) in Animal Feed. Combustion Method (990.03). *Official Methods of Analysis*, 16.

- Arogo, J., Westerman, P., & Heber, A. (2003). A review of ammonia emissions from confined swine feeding operations. *Transactions of the American Society of Agricultural Engineers*, *46*, 805–817. <https://doi.org/10.13031/2013.13597>
- Atakora, J. K. A., Moehn, S., & Ball, R. O. (2011). Enteric methane produced by finisher pigs is affected by dietary crude protein content of barley grain based, but not by corn based, diets. *Animal Feed Science and Technology*, *166–167*, 412–421. <https://doi.org/10.1016/j.anifeedsci.2011.04.029>
- Barrington, S., Choinière, D., Trigui, M., & Knight, W. (2002). Effect of carbon source on compost nitrogen and carbon losses. *Bioresource Technology*, *83*(3), 189–194. [https://doi.org/10.1016/S0960-8524\(01\)00229-2](https://doi.org/10.1016/S0960-8524(01)00229-2)
- Bernal, M. P., Albuquerque, J. A., & Moral, R. (2009). Composting of animal manures and chemical criteria for compost maturity assessment. A review. *Bioresource Technology*, *100*(22), 5444–5453. <https://doi.org/10.1016/j.biortech.2008.11.027>
- Broucek, J. (2016). Nitrous Oxide Production from Cattle and Swine Manure. *Journal of Animal Behaviour and Biometeorology*, *5*, 13–19. <https://doi.org/10.14269/2318-1265/jabb.v5n1p13-19>
- Brown-Brandl, T., Nienaber, J., Xin, H., & Gates, R. (2004). A Literature Review of Swine Heat Production. *Transaction of the ASAE*, *47*(1), 259–270. <https://doi.org/10.13031/2013.15867>
- Call, E., Bill, B., McLean, C., Call, N., Bernkopf, A., & Oberg, C. (2017). Hazardous Drug Contamination of Drug Preparation Devices and Staff: A Contamination Study Simulating the Use of Chemotherapy Drugs in a Clinical Setting. *Hospital Pharmacy*, *52*(8), Article 8. <https://doi.org/10.1177/0018578717722870>
- Calvet, S., Cambra-López, M., Blanes-Vidal, V., Estellés, F., & Torres, A. G. (2010). Ventilation rates in mechanically-ventilated commercial poultry buildings in Southern Europe: Measurement system development and uncertainty analysis. *Biosystems Engineering*, *106*(4), Article 4. <https://doi.org/10.1016/j.biosystemseng.2010.05.006>
- Camargo, J. A., & Alonso, A. (2006). Ecological and toxicological effects of inorganic nitrogen pollution in aquatic ecosystems: A global assessment. *Environment International*, *32*(6), 831–849. <https://doi.org/10.1016/j.envint.2006.05.002>
- Canh, T. T., Verstegen, M. W., Aarnink, A. J., & Schrama, J. W. (1997). Influence of dietary factors on nitrogen partitioning and composition of urine and feces of fattening pigs. *Journal of Animal Science*, *75*(3), 700–706. <https://doi.org/10.2527/1997.753700x>
- Cargo-Froom, C. (2022). *Pulses as alternative proteins for growing swine: An investigation into the effects of processing on pulse nutrient characterization and a comparison of key methodologies used to quantify protein quality in mammals* [University of Guelph]. <https://hdl.handle.net/10214/27256>
- CFSPH, ISU. (2013). *Routes of disease transmission*. http://www.cfsph.iastate.edu/Zoonoses_Textbook/Assets/transmission_routes_def_CA.pdf

- Chen, L., Lim, T.-T., Jin, Y., Heber, A. J., Ni, J.-Q., Cortus, E. L., & Kilic, I. (2014). Ventilation rate measurements at a mechanically-ventilated pig finishing quad barn. *Biosystems Engineering*, *121*, 96–104. <https://doi.org/10.1016/j.biosystemseng.2014.02.015>
- Christensen, K., & Thorbek, G. (1987). Methane excretion in the growing pig. *The British Journal of Nutrition*, *57*(3), 355–361. <https://doi.org/10.1079/bjn19870043>
- CIGR. (2002). *Fourth Report of Working Group on Climatization of Animal Houses: Heat and moisture production at animal and house levels* (4th ed.). Danish Institute of Agricultural Sciences.
- Colina, J., Lewis, A., & Miller, P. S. (2000). A Review of the Ammonia Issue and Pork Production. *Nebraska Swine Reports*. https://digitalcommons.unl.edu/coopext_swine/108
- Conover, D. M., & Gibson, K. E. (2017). Impact of soap type—Foaming vs. Gel-based—On handwashing time. *Food Control*, *73*, 878–882. <https://doi.org/10.1016/j.foodcont.2016.09.033>
- Cortus, E., Lemay, S., & Barber, E. (2010a). Dynamic Simulation of Ammonia Concentration and Emission within Swine Barns: Part I. Model Development. *Transactions of the ASABE*, *53*, 911–923. <https://doi.org/10.13031/2013.30074>
- Cortus, E., Lemay, S., & Barber, E. (2010b). Dynamic Simulation of Ammonia Concentration and Emission within Swine Barns: Part II. Model Calibration and Validation. *Transactions of the ASABE*, *53*, 925–938. <https://doi.org/10.13031/2013.30075>
- Cortus, E., Lemay, S. P., Barber, E. M., Hill, G. A., & Godbout, S. (2008). A dynamic model of ammonia emission from urine puddles. *Biosystems Engineering*, *99*(3), 390–402. <https://doi.org/10.1016/j.biosystemseng.2007.11.004>
- Coufal, C. D., Chavez, C., Niemeyer, P. R., & Carey, J. B. (2006). Nitrogen emissions from broilers measured by mass balance over eighteen consecutive flocks. *Poultry Science*, *85*(3), 384–391. <https://doi.org/10.1093/ps/85.3.384>
- Crosson, P., Shalloo, L., O'Brien, D., Lanigan, G. J., Foley, P. A., Boland, T. M., & Kenny, D. A. (2011). A review of whole farm systems models of greenhouse gas emissions from beef and dairy cattle production systems. *Animal Feed Science and Technology*, *166–167*, 29–45. <https://doi.org/10.1016/j.anifeedsci.2011.04.001>
- Dale, E., & Brown, C. (2013). *Zoonotic Diseases from Poultry*. *6*(2), 76–82.
- Davis, L. G., Weber, D., & Lemon, S. (1989). Horizontal Transmission of Hepatitis B Virus. *The Lancet*, *333*(8643), 889–893. [https://doi.org/10.1016/S0140-6736\(89\)92876-6](https://doi.org/10.1016/S0140-6736(89)92876-6)
- De Boer, H. C., & Wiersma, M. (2021). Thermophilic composting of the pack can reduce nitrogen loss from compost-bedded dairy barns. *Biosystems Engineering*, *210*, 20–32. <https://doi.org/10.1016/j.biosystemseng.2021.07.015>
- Dee, S., Deen, J., Cano, J. P., Batista, L., & Pijoan, C. (2006). Further evaluation of alternative air-filtration systems for reducing the transmission of Porcine

- reproductive and respiratory syndrome virus by aerosol. *Canadian Journal of Veterinary Research*, 70(3), 168–175.
- Dee, S., Deen, J., Rossow, K., Wiese, C., Otake, S., Joo, H. S., & Pijoan, C. (2002). Mechanical transmission of porcine reproductive and respiratory syndrome virus throughout a coordinated sequence of events during cold weather. *Canadian Journal of Veterinary Research*, 66(4), 232–239.
- Del Prado, A., Crosson, P., Olesen, J. E., & Rotz, C. A. (2013). Whole-farm models to quantify greenhouse gas emissions and their potential use for linking climate change mitigation and adaptation in temperate grassland ruminant-based farming systems. *Animal*, 7, 373–385. <https://doi.org/10.1017/S1751731113000748>
- Demmers, T. G. M., Phillips, V. R., Short, L. S., Burgess, L. R., Hoxey, R. P., & Wathes, C. M. (2001). Validation of Ventilation Rate Measurement Methods and the Ammonia Emission from Naturally Ventilated Dairy and Beef Buildings in the United Kingdom. *Journal of Agricultural Engineering Research*, 79(1), 107–116. <https://doi.org/10.1006/jaer.2000.0678>
- Doorn, M. J., Natschke, D. F., & Meeuwissen, P. C. (2002). *Review of Emission Factors and Methodologies to Estimate Ammonia Emissions from Animal Waste Handling*. U.S. Environmental Protection Agency. <http://nepis.epa.gov/Exe/ZyPURL.cgi?Dockey=2000E6XZ.txt>
- Driemer, J., & Van den Weghe, H. (1997). *Nitrous oxide emissions during nitrification and denitrification of pig manure* (J. Voermans & G. Monteny, Eds.; pp. 389–396). Dutch Society of Agricultural Engineering.
- Elzing, A., & Monteny, G. J. (1997a). Ammonia emission in a scale model of a dairy-cow house. *Transactions of the American Society of Agricultural Engineers*, 40(3), 713–720. Scopus.
- Elzing, A., & Monteny, G. J. (1997b). Modeling and experimental determination of ammonia emissions rates from a scale model dairy-cow house. *Transactions of the ASAE (USA)*. https://scholar.google.com/scholar_lookup?title=Modeling+and+experimental+determination+of+ammonia+emissions+rates+from+a+scale+model+dairy-cow+house&author=Elzing%2CA.+%28IMAG-DLO%2CWageningen%2C+The+Netherlands.%29&publication_year=1997
- Fangmeier, A., Hadwiger-Fangmeier, A., Van der Eerden, L., & Jäger, H.-J. (1994). Effects of atmospheric ammonia on vegetation—A review. *Environmental Pollution*, 86(1), 43–82. [https://doi.org/10.1016/0269-7491\(94\)90008-6](https://doi.org/10.1016/0269-7491(94)90008-6)
- Feddes, J., & DeShazer, J. (1991). Feed consumption as a parameter for establishing minimum ventilation rates. *Transaction of the ASAE*, 31(2), 571–575. <https://doi.org/10.13031/2013.30749>
- Fenske, R. A., Birnbaum, S. G., Methner, M. M., Lu, C., & Nigg, H. N. (2002). Fluorescent tracer evaluation of chemical protective clothing during pesticide applications in central Florida citrus groves. *Journal of Agricultural Safety and Health*, 8(3), 319–331. <https://doi.org/10.13031/2013.9056>

- Fiedler, M., Berg, W., Ammon, C., Loebstin, C., Sanftleben, P., Samer, M., von Bobrutzki, K., Kiwan, A., & Saha, C. K. (2013). Air velocity measurements using ultrasonic anemometers in the animal zone of a naturally ventilated dairy barn. *Biosystems Engineering*, *116*(3), 276–285. <https://doi.org/10.1016/j.biosystemseng.2012.10.006>
- Firestone, M., & Davidson, E. (1989). Microbiological Basis of NO and N₂O Production and Consumption in Soil. *Exchange of Trace Gases between Terrestrial Ecosystems and the Atmosphere*, 47.
- Flesch, T. K., Vergé, X. P. C., Desjardins, R. L., & Worth, D. (2013). Methane emissions from a swine manure tank in western Canada. *Canadian Journal of Animal Science*, *93*(1), 159–169. <https://doi.org/10.4141/cjas2012-072>
- Gates, R., Casey, K., Xin, H., Wheeler, E., & Simmons, J. (2004). Fan Assessment Numeration System (FANS) Design and Calibration Specifications. *Transactions of the ASAE. American Society of Agricultural Engineers*, *47*, 1709–1715. <https://doi.org/10.13031/2013.17613>
- Gerber, P. J., Steinfeld, H., Henderson, B., Mottet, A., Opio, C., Dijkman, J., Falcucci, A., & Tempio, G. (2013). *Tackling climate change through livestock: A global assessment of emissions and mitigation opportunities*. Food and Agriculture Organization of the United Nations (FAO). <https://www.fao.org/3/i3437e/i3437e.pdf>
- Groot Koerkamp, P. W. G., Metz, J. H. M., Uenk, G. H., Phillips, V. R., Holden, M. R., Sneath, R. W., Short, J. L., White, R. P. P., Hartung, J., Seedorf, J., Schröder, M., Linkert, K. H., Pedersen, S., Takai, H., Johnsen, J. O., & Wathes, C. M. (1998). Concentrations and Emissions of Ammonia in Livestock Buildings in Northern Europe. *Journal of Agricultural Engineering Research*, *70*(1), 79–95. <https://doi.org/10.1006/jaer.1998.0275>
- Grossi, G., Goglio, P., Vitali, A., & Williams, A. G. (2019). Livestock and climate change: Impact of livestock on climate and mitigation strategies. *Animal Frontiers*, *9*(1), 69–76. <https://doi.org/10.1093/af/vfy034>
- Halvorson, D. A., & Hueston, W. D. (2006). The Development of an Exposure Risk Index as a Rational Guide for Biosecurity Programs. *Avian Diseases*, *50*(4), 516–519. <https://doi.org/10.1637/7491-121405R2.1>
- Harrison, O., Dahmer, P., Gebhardt, J., Paulk, C., Woodworth, J., & Jones, C. (2022). Evaluation of biosecurity measures on a swine operation using Glo Germ powder as a visible learning aid. *Journal of Swine Health and Production*, *30*, 362–366. <https://doi.org/10.54846/jshap/1289>
- Hashimoto, A. G. (1972). *Ammonia Desorption from Concentrated Chicken Manure Slurries*. <https://primo.lib.umn.edu>
- Hassouna, M., Eglin, T., Cellier, P., Colomb, V., & Cohan, J.-P. (2016). *Measuring Emissions From Livestock Farming: Greenhouse gases, Ammonia and Nitrogen oxides*. INRA-ADEME. <https://hal.science/hal-01567208>

- Hinz, T., & Linke, S. (1998). A Comprehensive Experimental Study of Aerial Pollutants in and Emissions from Livestock Buildings. Part 1: Methods. *Journal of Agricultural Engineering Research*, 70(1), 111–118.
<https://doi.org/10.1006/jaer.1997.0279>
- Hoeksma, P., Verdoes, N., Oosthoek, J., & Voermans, J. A. M. (1992). Reduction of ammonia volatilization from pig houses using aerated slurry as recirculation liquid. *Livestock Production Science*, 31(1), 121–132.
[https://doi.org/10.1016/0301-6226\(92\)90060-H](https://doi.org/10.1016/0301-6226(92)90060-H)
- Hoff, S. J., Bundy, D. S., Nelson, M. A., Zelle, B. C., Jacobson, L. D., Heber, A. J., Ni, J., Zhang, Y., Koziel, J. A., & Beasley, D. B. (2006). Emissions of Ammonia, Hydrogen Sulfide, and Odor before, during, and after Slurry Removal from a Deep-Pit Swine Finisher. *Journal of the Air & Waste Management Association*, 56(5), 581–590. <https://doi.org/10.1080/10473289.2006.10464472>
- Hristov, A. N., Hanigan, M., Cole, A., Todd, R., McAllister, T. A., Ndegwa, P. M., & Rotz, A. (2011). Review: Ammonia emissions from dairy farms and beef feedlots. *Canadian Journal of Animal Science*, 91(1), 1–35.
<https://doi.org/10.4141/CJAS10034>
- Hu, E., Sutitarnnontr, P., Tuller, M., & Jones, S. B. (2018). Modeling temperature and moisture dependent emissions of carbon dioxide and methane from drying dairy cow manure. *Frontiers of Agricultural Science and Engineering*, 5(2), Article 2.
<https://doi.org/10.15302/J-FASE-2018215>
- Inbar, Y., Hadar, Y., & Chen, Y. (1993). Recycling of Cattle Manure: The Composting Process and Characterization of Maturity. *Journal of Environmental Quality*, 22(4), 857–863. <https://doi.org/10.2134/jeq1993.00472425002200040032x>
- IPCC, Calvo Buendia, E., Tanabe, K., Kranjc, A., Baasansuren, J., Fukuda, M., Ngarize, S., Osako, A., Pyrozhenko, Y., Shermanau, P., & Federici, S. (2019). Agriculture, Forestry, and Other Land Use. In *2019 Refinement to the 2006 IPCC Guidelines for National Greenhouse Gas Inventories* (Vol. 4). IPCC.
- JAOAC. (1996). Ash of Animal Feed (942.05) *Official Methods of Analysis*. 25, 857 (1942); 26, 220 (1943).
- Jeppsson, K.-H. (2000). SE—Structure and Environment: Carbon Dioxide Emission and Water Evaporation from Deep Litter Systems. *Journal of Agricultural Engineering Research*, 77(4), 429–440. <https://doi.org/10.1006/jaer.2000.0612>
- Jin, Y., Lim, T.-T., Ni, J.-Q., Ha, J.-H., & Heber, A. J. (2012). Emissions monitoring at a deep-pit swine finishing facility: Research methods and system performance. *Journal of the Air & Waste Management Association*, 62(11), 1264–1276.
<https://doi.org/10.1080/10962247.2012.707163>
- Jørgensen, H., Knudsen, K., Theil, P., & Peter. (2011). *Enteric Methane Emission from Pigs* (pp. 605–622). <https://doi.org/10.5772/24377>
- Jose, V. S., Sejian, V., Bagath, M., Ratnakaran, A. P., Lees, A. M., Al-Hosni, Y. A. S., Sullivan, M., Bhatta, R., & Gaughan, J. B. (2016). Modeling of Greenhouse Gas

- Emission from Livestock. *Frontiers in Environmental Science*, 4. <https://www.frontiersin.org/articles/10.3389/fenvs.2016.00027>
- Jung, K., Saif, L. J., & Wang, Q. (2020). Porcine epidemic diarrhea virus (PEDV): An update on etiology, transmission, pathogenesis, and prevention and control. *Virus Research*, 286, 198045. <https://doi.org/10.1016/j.virusres.2020.198045>
- Jungbluth, T., Hartung, E., & Brose, G. (2001). Greenhouse gas emissions from animal houses and manure stores. *Nutrient Cycling in Agroecosystems*, 60(1), 133–145. <https://doi.org/10.1023/A:1012621627268>
- Kaharabata, S. K., Schuepp, P. H., & Desjardins, R. L. (1998). Methane emissions from above ground open manure slurry tanks. *Global Biogeochemical Cycles*, 12(3), 545–554. <https://doi.org/10.1029/98GB01866>
- Kebreab, E., Clark, K., Wagner-Riddle, C., & France, J. (2006). Methane and nitrous oxide emissions from Canadian animal agriculture: A review. *Canadian Journal of Animal Science*, 86(2), 135–158. Scopus. <https://doi.org/10.4141/a05-010>
- Keener, H. M., & Zhao, L. (2008). A modified mass balance method for predicting NH₃ emissions from manure N for livestock and storage facilities. *Biosystems Engineering*, 99(1), Article 1. <https://doi.org/10.1016/j.biosystemseng.2007.09.006>
- Kirchgessner, M., Kreuzer, M., Mueller, H. L., & Windisch, W. (1991). Release of methane and of carbon dioxide by the pig. *Agribiological Research (Germany, F.R.)*. https://scholar.google.com/scholar_lookup?title=Release+of+methane+and+of+carbon+dioxide+by+the+pig&author=Kirchgessner%2C+M.+%28Technische+Univ.+Muenchen%2C+Freising-Weihenstephan+%28Germany%29.+Inst.+fuer+Ernaehrungsphysiologie%29&publication_year=1991
- Kirchmann, H., & Witter, E. (1989). Ammonia volatilization during aerobic and anaerobic manure decomposition. *Plant and Soil*, 115(1), 35–41. <https://doi.org/10.1007/BF02220692>
- Koelsch, R., & Stowell, R. (2005). *Ammonia Emissions Estimator*. University of Nebraska. <https://www.agric.gov.ab.ca/app19/calc/ammonia/KoelschAmmoniaEmissionsEstimator.pdf>
- Korzukhin, M. D., Ter-Mikaelian, M. T., & Wagner, R. G. (1996). Process versus empirical models: Which approach for forest ecosystem management? *Canadian Journal of Forest Research*, 26(5), 879–887. <https://doi.org/10.1139/x26-096>
- Koziel, J., Aneja, V., & Baek, B.-H. (2006). Gas-to-Particle Conversion Process between Ammonia, Acid Gases, and Fine Particles in the Atmosphere. *Animal Agriculture and the Environment: National Center for Manure and Animal Waste Management White Papers*, 201–224. <https://doi.org/10.13031/2013.20254>
- Lewis, A. J., & Southern, L. L. (2000). *Swine Nutrition*. CRC Press. <https://doi.org/10.1201/9781420041842>

- Leytem, A. B., Bjorneberg, D. L., Koehn, A. C., Moraes, L. E., Kebreab, E., & Dungan, R. S. (2017). Methane emissions from dairy lagoons in the western United States. *Journal of Dairy Science*, *100*(8), 6785–6803. <https://doi.org/10.3168/jds.2017-12777>
- Li, C., Salas, W., Zhang, R., Krauter, C., Rotz, A., & Mitloehner, F. (2012). Manure-DNDC: A biogeochemical process model for quantifying greenhouse gas and ammonia emissions from livestock manure systems. *Nutrient Cycling in Agroecosystems*, *93*(2), 163–200. <https://doi.org/10.1007/s10705-012-9507-z>
- Li, H., Xin, H., & Burns, R. (2010). The Uncertainty of Nitrogen Mass Balance for Turkey Housing. *Iowa State University Animal Industry Report*, *7*(1). https://doi.org/10.31274/ans_air-180814-160
- Lorimor, J., Powers, W., & Sutton, A. (2004). *Manure Characteristics—Manure Management System Series* (2nd ed.). <https://store.extension.iastate.edu/product/Manure-Characteristics-Manure-Management-System-Series>
- Lyu, Z., Shao, N., Akinyemi, T., & Whitman, W. B. (2018). Methanogenesis. *Current Biology*, *28*(13), R727–R732. <https://doi.org/10.1016/j.cub.2018.05.021>
- MacLeod, M. J., Vellinga, T., Opio, C., Falcucci, A., Tempio, G., Henderson, B., Makkar, H., Mottet, A., Robinson, T., Steinfeld, H., & Gerber, P. J. (2018). Invited review: A position on the Global Livestock Environmental Assessment Model (GLEAM). *Animal*, *12*(2), 383–397. <https://doi.org/10.1017/S1751731117001847>
- Maitland, J., Boyer, R., Gallagher, D., Duncan, S., Bauer, N., Kause, J., & Eifert, J. (2013). Tracking Cross-Contamination Transfer Dynamics at a Mock Retail Deli Market Using GloGerm. *Journal of Food Protection*, *76*(2), Article 2. <https://doi.org/10.4315/0362-028X.JFP-12-271>
- Martin, M. (2017). Biosecurity and Disease Control—The Problems Defined. In *A Practical Guide for Managing Risk in Poultry Production*. American Association of Avian Pathologists, Inc.
- Meegoda, J. N., Li, B., Patel, K., & Wang, L. B. (2018). A Review of the Processes, Parameters, and Optimization of Anaerobic Digestion. *International Journal of Environmental Research and Public Health*, *15*(10), 2224. <https://doi.org/10.3390/ijerph15102224>
- Mobley, H., & Hausinger, R. (1989). Microbial ureases: Significance, regulation, and molecular characterization. *Microbiological Reviews*, *53*(1), 85–108. <https://doi.org/10.1128/mr.53.1.85-108.1989>
- Moehn, S., Price, J. D., Zijlstra, R. T., Sauer, W. C., Clark, O., Ball, R. O., Atakora, J. K. A., Feddes, J. J., Zhang, Y., Leonard, J. J., Edeogu, I., & Morin, B. (2005). Diet Manipulation to Control Odor and Gas Emissions from Swine Production. In *Climate Change and Managed Ecosystems* (pp. 295–316). <https://doi.org/10.1201/9780849330971.ch15>

- Møller, H. B., Sommer, S. G., & Ahring, B. K. (2004). Biological Degradation and Greenhouse Gas Emissions during Pre-Storage of Liquid Animal Manure. *Journal of Environmental Quality*, 33(1), 27–36. Scopus.
<https://doi.org/10.2134/jeq2004.2700>
- Monteny, G. J., Schulte, D. D., Elzing, A., & Lamaker, E. J. J. (1998). A conceptual mechanistic model for the ammonia emissions from free stall cubicle dairy cow houses. *Transactions of the ASAE*, 41(1), 193–201.
- Müller, W., & Schneider, B. (1985). On the issue of heat, water vapor and CO₂ accumulation in dairy cattle and pig fattening stables. Part 1. Provisional planning data for the use of heat exchangers and heat pumps in livestock housing. *Veterinary Review*, 40(4), 274–280.
- National Research Council. (1989). Protein and Amino Acids. In *Recommended Dietary Allowances: 10th Edition* (Vol. 6). National Academies Press (US).
<https://www.ncbi.nlm.nih.gov/books/NBK234922/>
- Nelson, N. P., Weng, M., Hofmeister, M., Moore, K., Doshani, M., Kamili, S., Koneru, A., Haber, P., Hagan, L., Romero, J., Schillie, S., & Harris, A. (2020). Prevention of Hepatitis A Virus Infection in the United States: Recommendations of the Advisory Committee on Immunization Practices, 2020. *Recommendations of the Advisory Committee on Immunization Practices*, 69(5).
<https://doi.org/10.15585/mmwr.rr6905a1>
- Ni, J. (1999). Mechanistic Models of Ammonia Release from Liquid Manure: A Review. *Journal of Agricultural Engineering Research*, 72(1), 1–17.
<https://doi.org/10.1006/jaer.1998.0342>
- Ni, J., Heber, A., Sutton, A., & Kelly, D. (2009). Mechanisms of Gas Releases from Swine Wastes. *Transactions of the ASABE*, 52, 2013–2025.
<https://doi.org/10.13031/2013.29203>
- Ni, J., Hendriks, J., Coenegrachts, J., & Vinckier, C. (1999). Production of carbon dioxide in a fattening pig house under field conditions. I. Exhalation by pigs. *Atmospheric Environment*, 33(22), 3691–3696. [https://doi.org/10.1016/S1352-2310\(99\)00127-2](https://doi.org/10.1016/S1352-2310(99)00127-2)
- Ni, J., Vinckier, C., Hendriks, J., & Coenegrachts, J. (1999). Production of carbon dioxide in a fattening pig house under field conditions. II. Release from the manure. *Atmospheric Environment*, 33(22), 3697–3703.
[https://doi.org/10.1016/S1352-2310\(99\)00128-4](https://doi.org/10.1016/S1352-2310(99)00128-4)
- Noblet, J., Dourmad, J. Y., Le Dividich, J., & Dubois, S. (1989). Effect of ambient temperature and addition of straw or alfalfa in the diet on energy metabolism in pregnant sows. *Livestock Production Science*, 21(4), 309–324.
[https://doi.org/10.1016/0301-6226\(89\)90091-2](https://doi.org/10.1016/0301-6226(89)90091-2)
- Noblet, J., & Shi, X. S. (1994). Effect of body weight on digestive utilization of energy and nutrients of ingredients and diets in pigs. *Livestock Production Science*, 37, 323–338. [https://doi.org/10.1016/0301-6226\(94\)90126-0](https://doi.org/10.1016/0301-6226(94)90126-0)

- Noël, S., Weigel, K., Bramstedt, K., Rozanov, A., Weber, M., Bovensmann, H., & Burrows, J. P. (2018). Water vapour and methane coupling in the stratosphere observed using SCIAMACHY solar occultation measurements. *Atmospheric Chemistry and Physics*, 18(7), 4463–4476. <https://doi.org/10.5194/acp-18-4463-2018>
- Okrouhlá, M., Stupka, R., Čítek, J., Šprysl, E., Trnka, M., & Štolc, L. (2006). Amino acid composition of pig meat in relation to live weight and sex. *Czech Journal of Animal Science*, 51. <https://doi.org/10.17221/3974-CJAS>
- Okrouhlá, M., Stupka, R., Čítek, J., Šprysl, M., Kluzáková, E., Trnka, M., & Štolc, L. (2006). Amino acid composition of pig meat in relation to live weight and sex. *Czech Journal of Animal Science*, 51(12), 529–534. <https://doi.org/10.17221/3974-CJAS>
- Olesen, J., Schelde, K., Weiske, A., Weisbjerg, M., Asman, W. A. H., & Djurhuus, J. (2006). Modelling greenhouse gas emissions from European conventional and organic dairy farms. *Agriculture, Ecosystems & Environment*, 112, 207–220. <https://doi.org/10.1016/j.agee.2005.08.022>
- Olesen, J., & Sommer, S. G. (1993). Modelling effects of wind speed and surface cover on ammonia volatilization from stored pig slurry. *Atmospheric Environment. Part A. General Topics*, 27(16), 2567–2574. [https://doi.org/10.1016/0960-1686\(93\)90030-3](https://doi.org/10.1016/0960-1686(93)90030-3)
- Park, K.-H., Wagner-Riddle, C., & Gordon, R. J. (2010). Comparing methane fluxes from stored liquid manure using micrometeorological mass balance and floating chamber methods. *Agricultural and Forest Meteorology*, 150(2), 175–181. <https://doi.org/10.1016/j.agrformet.2009.09.013>
- Pedersen, S., Blanes-Vidal, V., Joergensen, H., Chwalibog, A., Haeussermann, A., Heetkamp, M. J. W., & Aarnink, A. J. A. (2008). Carbon Dioxide Production in Animal Houses: A literature review. *Agricultural Engineering International*, X(BC 08 008), Article BC 08 008.
- Peiris, J. S. M., de Jong, M. D., & Guan, Y. (2007). Avian Influenza Virus (H5N1): A Threat to Human Health. *Clinical Microbiology Reviews*, 20(2), 243–267. <https://doi.org/10.1128/cmr.00037-06>
- Pescod, M. B. (1996). The role and limitations of anaerobic pond systems. *Water Science and Technology*, 33(7), 11–21. <https://doi.org/10.2166/wst.1996.0117>
- Philippe, F.-X., & Nicks, B. (2015). Review on greenhouse gas emissions from pig houses: Production of carbon dioxide, methane and nitrous oxide by animals and manure. *Agriculture, Ecosystems & Environment*, 199, 10–25. <https://doi.org/10.1016/j.agee.2014.08.015>
- Phillips, V. R., Scholtens, R., Lee, D., Garland, J. A., & Sneath, R. W. (2001). A review of methods for measuring emission rates of ammonia from livestock buildings and slurry or manure stores, Part 1: Assessment of basic approaches. *Journal of Agricultural Engineering Research*, 77(4), 355–364.

- Poth, M., & Focht, D. D. (1985). 15N Kinetic Analysis of N₂O Production by *Nitrosomonas europaea*: An Examination of Nitrifier Denitrification. *Applied and Environmental Microbiology*, 49(5), 1134–1141.
<https://doi.org/10.1128/aem.49.5.1134-1141.1985>
- Qu, Q., Groot, J. C. J., Zhang, K., & Schulte, R. P. O. (2021). Effects of housing system, measurement methods and environmental factors on estimating ammonia and methane emission rates in dairy barns: A meta-analysis. *Biosystems Engineering*, 205, 64–75. Scopus. <https://doi.org/10.1016/j.biosystemseng.2021.02.012>
- Ranjan, R., & Singh, S. P. (2023). Removal of Urea and Ammonia from Wastewater. In A. Sinha, S. P. Singh, & A. B. Gupta (Eds.), *Persistent Pollutants in Water and Advanced Treatment Technology* (pp. 335–353). Springer Nature.
https://doi.org/10.1007/978-981-99-2062-4_14
- Reay, D. S., Smith, P., Christensen, T. R., James, R. H., & Clark, H. (2018). Methane and Global Environmental Change. *Annual Review of Environment and Resources*, 43, 165–192.
- Rigolot, C., Espagnol, S., Robin, P., Hassouna, M., Béline, F., Paillat, J. M., & Dourmad, J.-Y. (2010). Modelling of manure production by pigs and NH₃, N₂O and CH₄ emissions. Part II: Effect of animal housing, manure storage and treatment practices. *Animal: An International Journal of Animal Bioscience*, 4(8), 1413–1424. <https://doi.org/10.1017/S1751731110000509>
- Ritz, C. W., Fairchild, B. D., & Lacy, M. P. (2004). Implications of Ammonia Production and Emissions from Commercial Poultry Facilities: A Review. *Journal of Applied Poultry Research*, 13(4), 684–692. <https://doi.org/10.1093/japr/13.4.684>
- Rotz, C. A., Montes, F., Hafner, S. D., Heber, A. J., & Grant, R. H. (2014). Ammonia Emission Model for Whole Farm Evaluation of Dairy Production Systems. *Journal of Environmental Quality*, 43(4), 1143–1158.
<https://doi.org/10.2134/jeq2013.04.0121>
- Schauberger, G., Lim, T.-T., Ni, J.-Q., Bundy, D. S., Haymore, B. L., Diehl, C. A., Duggirala, R. K., & Heber, A. J. (2013). Empirical model of odor emission from deep-pit swine finishing barns to derive a standardized odor emission factor. *Atmospheric Environment*, 66, 84–90.
<https://doi.org/10.1016/j.atmosenv.2012.05.046>
- Schindelin, J., Arganda-Carreras, I., Frise, E., Kaynig, V., Longair, M., Pietzsch, T., Preibisch, S., Rueden, C., Saalfeld, S., Schmid, B., Tinevez, J.-Y., White, D. J., Hartenstein, V., Eliceiri, K., Tomancak, P., & Cardona, A. (2012). Fiji: An open-source platform for biological-image analysis. *Nature Methods*, 9(7), Article 7.
<https://doi.org/10.1038/nmeth.2019>
- Solomon, S., Qin, D., Manning, M., Chen, Z., Marquis, M., Averyt, K. B., Tignor, M., & Miller, H. L. (2007). *Contribution of Working Group I to the Fourth Assessment Report of the Intergovernmental Panel on Climate Change* (IPCC Fourth Assessment Report). Intergovernmental Panel on Climate Change.
https://archive.ipcc.ch/publications_and_data/ar4/wg1/en/contents.html

- Sommer, S. G., Générmont, S., Cellier, P., Hutchings, N. J., Olesen, J. E., & Morvan, T. (2003). Processes controlling ammonia emission from livestock slurry in the field. *European Journal of Agronomy*, *19*(4), 465–486. [https://doi.org/10.1016/S1161-0301\(03\)00037-6](https://doi.org/10.1016/S1161-0301(03)00037-6)
- Sweeten, J. M., Fulhage, C., & Humenik, F. J. (1981). Methane Gas from Swine Manure. In *Pork Industry Handbook* (p. 4). Michigan State University Extension Service.
- U.S. EPA. (2020). *Development of Emissions Estimating Methodologies for Swine Barns and Lagoons: Draft*. https://www.epa.gov/sites/default/files/2020-08/documents/development_of_emissions_estimating_methodologies_for_swine_barns_and_lagoons.pdf
- USDA, APHIS. (2017). *HPAI response plan: The red book*.
- van der Goot, J. A., de Jong, M. C. M., Koch, G., & Van Boven, M. (2003). Comparison of the transmission characteristics of low and high pathogenicity avian influenza A virus (H5N2). *Epidemiology and Infection*, *131*(2), 1003–1013. <https://doi.org/10.1017/s0950268803001067>
- VanderZaag, A. C., Baldé, H., Habtewold, J., Le Riche, E. L., Burt, S., Dunfield, K., Gordon, R. J., Jenson, E., & Desjardins, R. L. (2019). Intermittent agitation of liquid manure: Effects on methane, microbial activity, and temperature in a farm-scale study. *Journal of the Air & Waste Management Association*, *69*(9), 1096–1106. <https://doi.org/10.1080/10962247.2019.1629359>
- VanderZaag, A. C., Flesch, T. K., Desjardins, R. L., Baldé, H., & Wright, T. (2014). Measuring methane emissions from two dairy farms: Seasonal and manure-management effects. *Agricultural and Forest Meteorology*, *194*, 259–267. <https://doi.org/10.1016/j.agrformet.2014.02.003>
- Van't Klooster, C. E., & Heitlager, B. P. (1994). Determination of Minimum Ventilation Rate in Pig Houses with Natural Ventilation based on Carbon Dioxide Balance. *Journal of Agricultural Engineering Research*, *57*(4), 279–287. <https://doi.org/10.1006/jaer.1994.1028>
- Wang-Li, L., Li, Q.-F., Wang, K., Bogan, B., Ni, J.-Q., Cortus, E., & Heber, A. (2013). The National Air Emissions Monitoring Study's Southeast Layer Site: Part I. Site Characteristics and Monitoring Methodology. *Transactions of the ASABE (American Society of Agricultural and Biological Engineers)*, *56*, 56–1157. <https://doi.org/10.13031/trans.56.9570>
- Welty, J., Wicks, C. E., & Wilson, R. E. (1984). *Fundamentals of Momentum, Heat, and Mass Transfer, 3rd Edition* (3rd edition). Wiley.
- West, J. J., & Fiore, A. M. (2005). Management of Tropospheric Ozone by Reducing Methane Emissions. *Environmental Science & Technology*, *39*(13), 4685–4691. <https://doi.org/10.1021/es048629f>
- Wilson, M. L., Cortus, S., Brimmer, R., Floren, J., Gunderson, L., Hicks, K., ... & Vocasek, F. (2022). *Recommended Methods of Manure Analysis*. University of Minnesota Libraries Publishing.

- Wolter, M., Prayitno, S., & Schuchardt, F. (2004). Greenhouse gas emission during storage of pig manure on a pilot scale. *Bioresource Technology*, 95(3), 235–244. <https://doi.org/10.1016/j.biortech.2003.01.003>
- Xing, Y.-F., Xu, Y.-H., Shi, M.-H., & Lian, Y.-X. (2016). The impact of PM_{2.5} on the human respiratory system. *Journal of Thoracic Disease*, 8(1), E69–E74. <https://doi.org/10.3978/j.issn.2072-1439.2016.01.19>
- Yang, P., Lorimor, J., & Xin, H. (2000). Nitrogen Losses from Laying Hen Manure in Commercial High-rise Layer Facilities. *Transactions of the ASAE*, 43(6), 1771–1780. <https://doi.org/10.13031/2013.3080>

Appendix

Table A1. Camera settings used for Canon EOS Rebel SL1 in Test Series 1-5.

Mode	Manual
Shutter Speed	1/250
Aperture	F7.1 for paper F11 for plastic and rubber
ISO	800
Exposure comp./AEB setting	0
Flash exposure comp	0
Picture style	Standard
White Balance	Auto
Auto-correct image brightness and contrast	Disabled
Metering Mode	Center-weighted average
Focus	Manual
Shooting	Single
Image Quality	High Quality JPEG
Lens	EFS 18-55 mm MF Stabilizer off Set at 18 mm

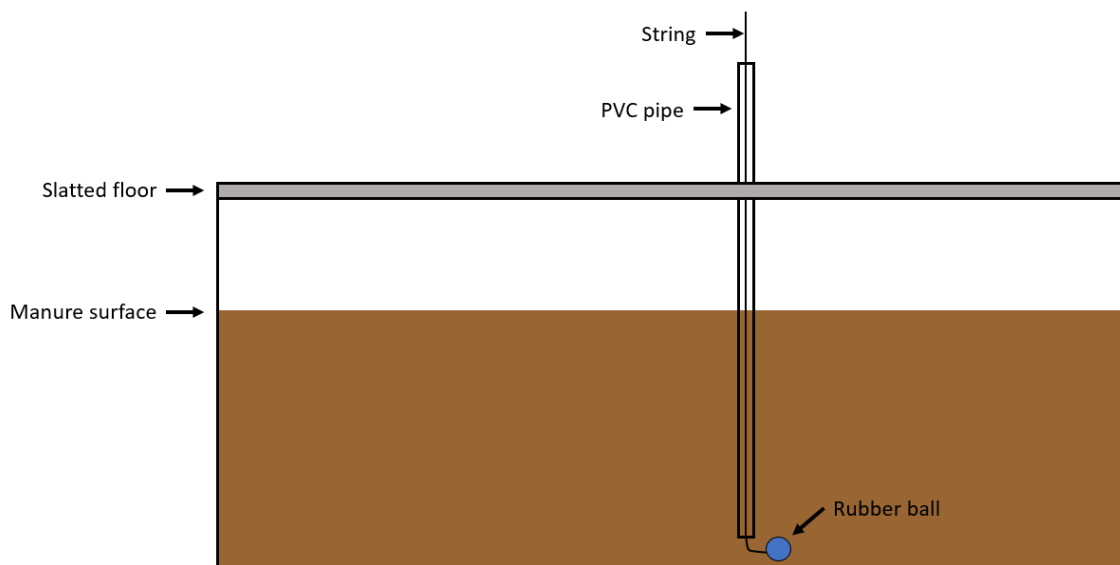


Figure A1. Graphical depiction of manure sampling methods.

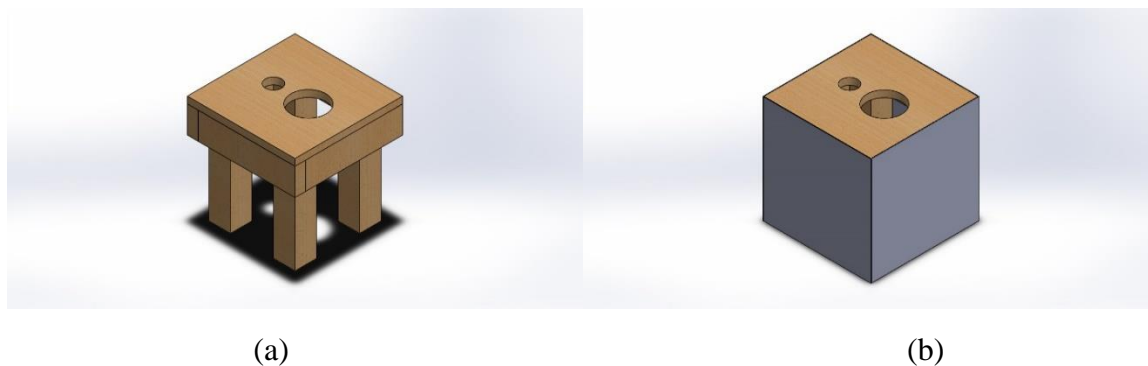


Figure A2. *Curtained table model constructed from wood without (a) and with (b) curtains made from blackout fabric lining. The fabric was secured using Velcro strips. The smaller hole was used for the UV light and the larger hole for the camera lens.*

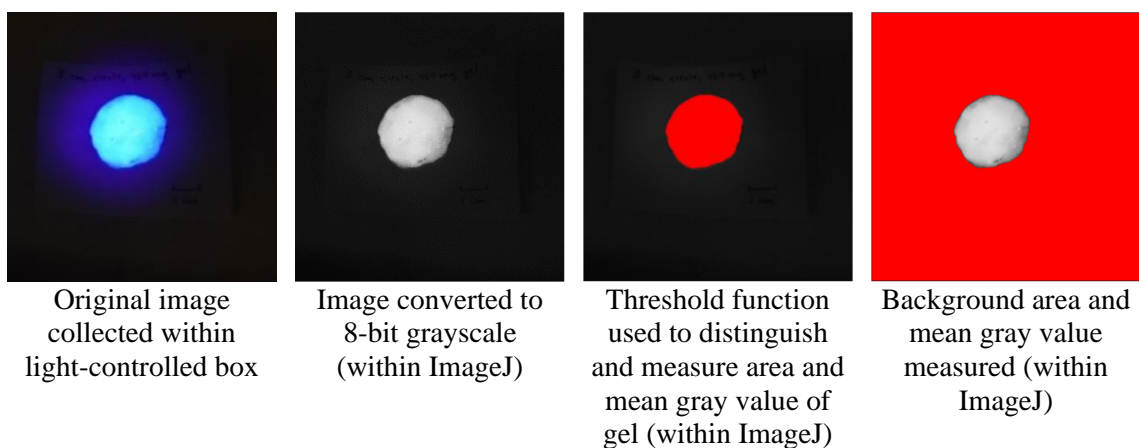


Figure A3. *The image analysis process to quantify the fluorescent luminance and the area containing fluoresced pixels for a circle of Glogerm™ gel on a paper, using ImageJ; method adapted from Schindelin et al. (2012).*